Coupled Electron-Ion Monte Carlo Method

Carlo Pierleoni

Physics Department, University of L'Aquila, Italy

Collaborations

- David M. Ceperley, UIUC, Illinois USA

- Mark Dewing, INTEL CORP., Champaign Illinois, USA
- Markus Holzmann, LPTCM, Paris VI, France.
- Kris Delaney, UIUC, Illinois USA.

Acknowledgments

CECAM for his hospitality
NCSA (USA) and CINECA (Italy) for computer time.

Outline

- Motivations
  - Beyond DFT
  - High pressure hydrogen: phase diagram and MIT

Outline

- Motivations
  - Beyond DFT
  - High pressure hydrogen: phase diagram and MIT
- Coupled Electron-Ion Monte Carlo (CEIMC)
  - Finite temperature Ions: Noisy Monte Carlo The Penalty Method
  - Ground state electrons:
    - VMC & RQMC
    - Moving the electrons: the bounce algorithm
    - Energy difference methods
    - Trial wave functions for hydrogen
    - Finite size effects: Twist Average Boundary Conditions (TABC)
  - Strategy for Protonic PIMC within CEIMC

Outline

- Motivations
  - Beyond DFT
  - High pressure hydrogen: phase diagram and MIT
- Coupled Electron-Ion Monte Carlo (CEIMC)
  - Finite temperature Ions: Noisy Monte Carlo The Penalty Method
  - Ground state electrons:
    - VMC & RQMC
    - Moving the electrons: the bounce algorithm
    - Energy difference methods
    - Trial wave functions for hydrogen
    - Finite size effects: Twist Average Boundary Conditions (TABC)
  - Strategy for Protonic PIMC within CEIMC
- Application: High pressure hydrogen
  - Atomic-metallic phase: EOS and proton melting
  - Molecular phase: preliminary results
  - Liquid-Liquid Phase Transition

Outline

- Motivations
  - Beyond DFT
  - High pressure hydrogen: phase diagram and MIT
- Coupled Electron-Ion Monte Carlo (CEIMC)
  - Finite temperature Ions: Noisy Monte Carlo The Penalty Method
  - Ground state electrons:
    - VMC & RQMC
    - Moving the electrons: the bounce algorithm
    - Energy difference methods
    - Trial wave functions for hydrogen
    - Finite size effects: Twist Average Boundary Conditions (TABC)
  - Strategy for Protonic PIMC within CEIMC
- Application: High pressure hydrogen
  - Atomic-metallic phase: EOS and proton melting
  - Molecular phase: preliminary results
  - Liquid-Liquid Phase Transition
- Future developments

motivations: beyond DFT

- Modern *AB-INITIO* simulation methods are largely based on Density Functional Theory (DFT), in principle exact but in practice it invokes the Local Density Approximation (LDA and various improvements GGA).
- DFT+LDA(GGA) is in general a good compromise between accuracy and efficiency to perform dynamical studies of several hundreds atoms for times of the order of *100 psec* (Car-Parrinello and BO Molecular Dynamics).
- There are cases in which DFT is not accurate enough (Van-der-Waals bonding systems, sp-bonded materials, calculation of excitation energies and energy gaps)
- Can we do better than DFT? Quantum Monte Carlo (QMC) provides in general better electronic energies for given ionic positions.

Carbon cluster C_{20}

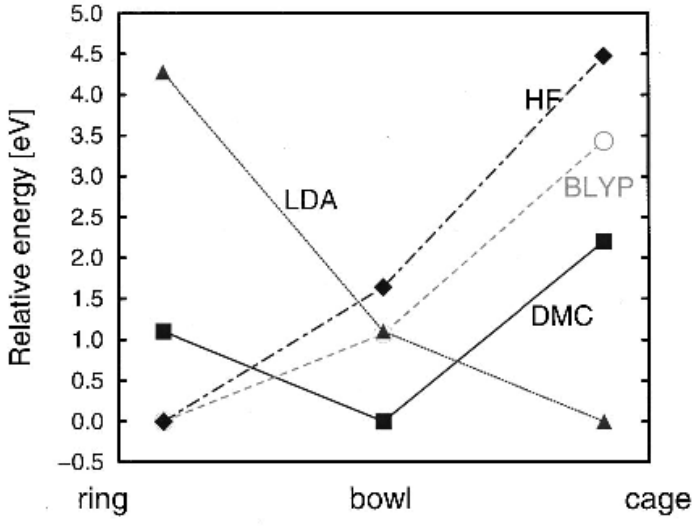

FIG. 15. Relative energies of C_{20} isomers from the HF, LDA, BLYP, and DMC methods. The energies are given relative to the lowest-energy isomer within the given theory. From Grossman, Mitas, and Raghavachari, 1995.

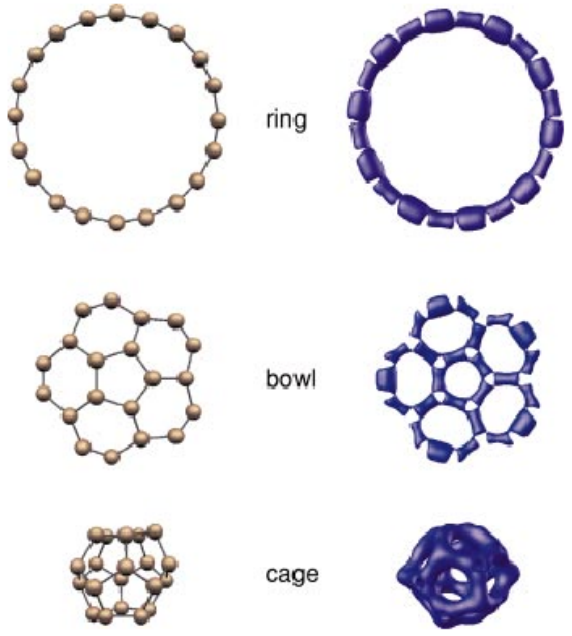

FIG. 14. Geometries and charge densities of C_{20} isomers calculated using the HF method. From Grossman, Mitas, and Raghavachari, 1995 [Color].

- J.C.Grossman et al. PRL, **75**, 3870 (1995).
- BLYP=Becke-Lee-Yang-Parr GGA
- Highly accurate chemical methods calculations confirms QMC data (R.B.Murphy, R.A.Friesner, Chem.Phys.Lett. **288**, 403 (1998))

beyond DFT

- Can we devise an efficient method to exploit the accuracy of QMC in *AB-INITIO* "dynamical" simulation of condensed systems?

beyond DFT

- Can we devise an efficient method to exploit the accuracy of QMC in *AB-INITIO* "dynamical" simulation of condensed systems?
- Previous attempts
  - Diffusion Monte Carlo for electrons and nuclei (DMC)
    (Ceperley-Alder 1987)
    - temperature effects are absent
    - time scale separation problem (even for hydrogen!)
  - Restricted Path Integral Monte Carlo (RPIMC)
    (Pierleoni, Ceperley et al, 1994, Militzer and Ceperley 1999)
    - electrons and nuclei are at finite temperature
    - sampling problem at low temperature ($T < 1/20 T_F$)

beyond DFT

- Can we devise an efficient method to exploit the accuracy of QMC in *AB-INITIO* "dynamical" simulation of condensed systems?
- Previous attempts
  - Diffusion Monte Carlo for electrons and nuclei (DMC)
    (Ceperley-Alder 1987)
    - temperature effects are absent
    - time scale separation problem (even for hydrogen!)
  - Restricted Path Integral Monte Carlo (RPIMC)
    (Pierleoni, Ceperley et al, 1994, Militzer and Ceperley 1999)
    - electrons and nuclei are at finite temperature
    - sampling problem at low temperature ($T < 1/20 T_F$)
- Coupled Electron-Ion Monte Carlo (CEIMC)

  - Born-Oppenheimer separation of time scales:
  ground state electrons, finite T nuclei

High pressure hydrogen

- The most abundant element in the universe : giant planets (>90%)
- The simplest element in the periodic table: good theoretical playground
- Still so much unknown!! The high pressure phases are still largely out of the experimental reach.

Hydrogen: phase diagram

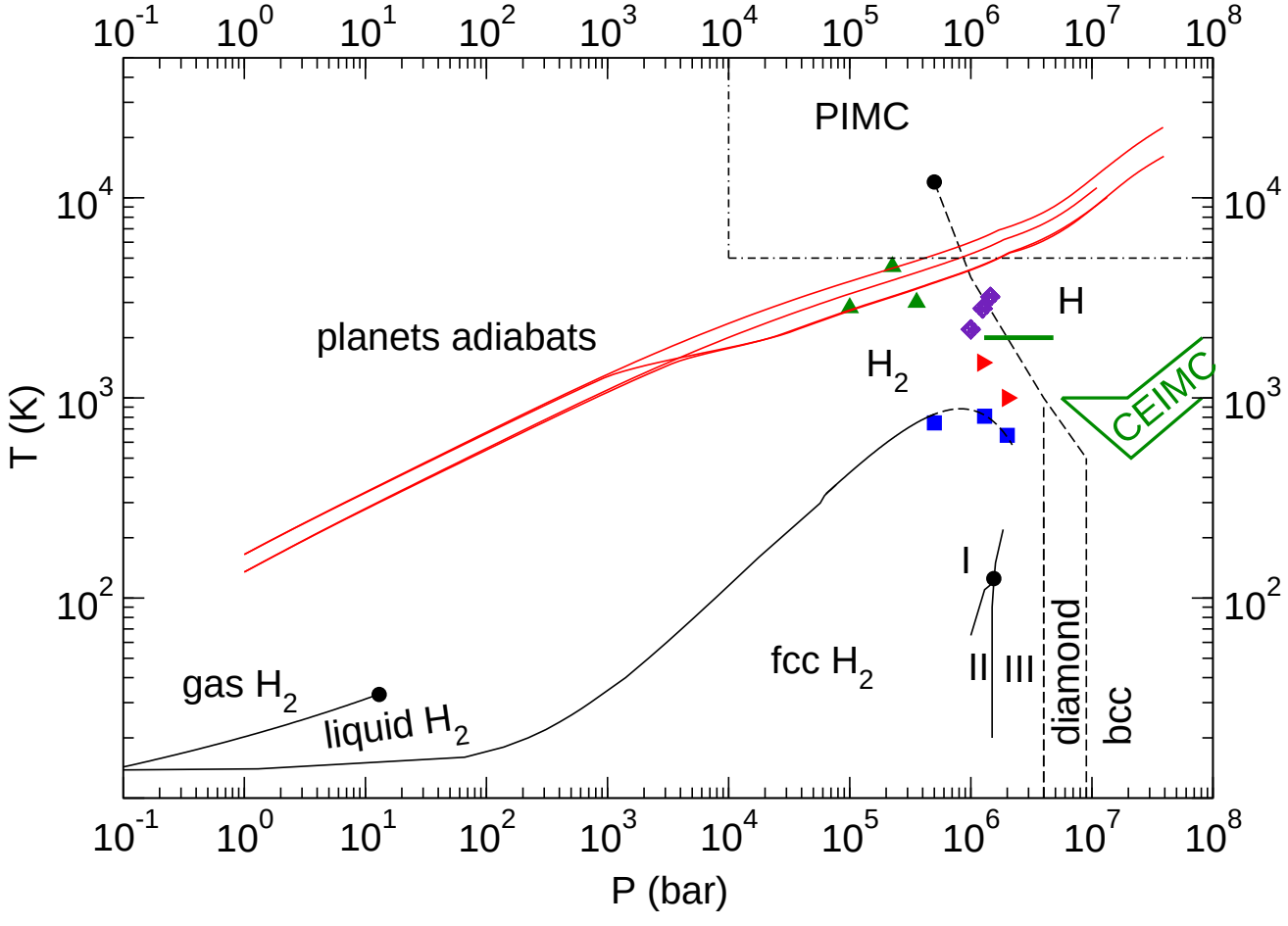

Hydrogen phase diagram. Continuous transition lines are experimental results, dashed lines are theoretical prediction from various methods. Blue squares and red right-triangle are ab-initio MD predictions of molecular melting (Bonev et al, Nature '04) and molecular dissociation in the liquid phase (Scandolo, PNAS '03). The diamonds are shock-waves experimental data through the liquid metalization (Weir et al. PRB '96). The green triangles are early CEIMC data for the insulating molecular state while the green domain on the extreme right indicates the CEIMC prediction for the melting (Pierleoni et al PRL '04). Red lines are model adiabats for the interior of the giant planets of the solar system.

Hydrogen: know and less know facts

- Solid hydrogen is insulating up to 3.5Mbars (DAC experiments, Loubeyre Nature ’02)

Hydrogen: know and less know facts

- Solid hydrogen is insulating up to 3.5Mbars (DAC experiments, Loubeyre Nature ’02)
- at T=0K molecular dissociation occurs at r_s=1.31 (DMC, Ceperley Alder PRB ’87)

Hydrogen: know and less know facts

- Solid hydrogen is insulating up to 3.5Mbars (DAC experiments, Loubeyre Nature '02)
- at T=0K molecular dissociation occurs at r_s=1.31 (DMC, Ceperley Alder PRB '87)
- At the molecular dissociation a diamond structure of protons is predicted. At higher pressure a diamond–bcc transition is expected (DMC, Natoli et al PRL '93).

Hydrogen: know and less know facts

- Solid hydrogen is insulating up to 3.5Mbars (DAC experiments, Loubeyre Nature ’02)
- at T=0K molecular dissociation occurs at r_s=1.31 (DMC, Ceperley Alder PRB ’87)
- At the molecular dissociation a diamond structure of protons is predicted. At higher pressure a diamond–bcc transition is expected (DMC, Natoli et al PRL ’93).
- crystal structures of different symmetry can have very close energies: needs of very accurate total energy methods.

Hydrogen: know and less know facts

- Solid hydrogen is insulating up to 3.5Mbars (DAC experiments, Loubeyre Nature '02)
- at T=0K molecular dissociation occurs at r_s=1.31 (DMC, Ceperley Alder PRB '87)
- At the molecular dissociation a diamond structure of protons is predicted. At higher pressure a diamond–bcc transition is expected (DMC, Natoli et al PRL '93).
- crystal structures of different symmetry can have very close energies: needs of very accurate total energy methods.
- Size effects are crucial to obtain accurate energies (Brillouin zone sampling in CPMD).

Hydrogen: know and less know facts

- Solid hydrogen is insulating up to 3.5Mbars (DAC experiments, Loubeyre Nature '02)
- at T=0K molecular dissociation occurs at r_s=1.31 (DMC, Ceperley Alder PRB '87)
- At the molecular dissociation a diamond structure of protons is predicted. At higher pressure a diamond–bcc transition is expected (DMC, Natoli et al PRL '93).
- crystal structures of different symmetry can have very close energies: needs of very accurate total energy methods.
- Size effects are crucial to obtain accurate energies (Brillouin zone sampling in CPMD).
- ZPM is large and favors isotropic structures (Kitamura et al, Nature 2000).

Hydrogen: know and less know facts

- Solid hydrogen is insulating up to 3.5Mbars (DAC experiments, Loubeyre Nature '02)
- at T=0K molecular dissociation occurs at r_s=1.31 (DMC, Ceperley Alder PRB '87)
- At the molecular dissociation a diamond structure of protons is predicted. At higher pressure a diamond–bcc transition is expected (DMC, Natoli et al PRL '93).
- crystal structures of different symmetry can have very close energies: needs of very accurate total energy methods.
- Size effects are crucial to obtain accurate energies (Brillouin zone sampling in CPMD).
- ZPM is large and favors isotropic structures (Kitamura et al, Nature 2000).
- Molecular phases I and II are understood, phase III is still unsettled.

Hydrogen: know and less know facts

- Solid hydrogen is insulating up to 3.5Mbars (DAC experiments, Loubeyre Nature '02)
- at T=0K molecular dissociation occurs at r_s=1.31 (DMC, Ceperley Alder PRB '87)
- At the molecular dissociation a diamond structure of protons is predicted. At higher pressure a diamond–bcc transition is expected (DMC, Natoli et al PRL '93).
- crystal structures of different symmetry can have very close energies: needs of very accurate total energy methods.
- Size effects are crucial to obtain accurate energies (Brillouin zone sampling in CPMD).
- ZPM is large and favors isotropic structures (Kitamura et al, Nature 2000).
- Molecular phases I and II are understood, phase III is still unsettled.
- Predicting metalization requires going beyond DFT-LDA-GGA (Johnson Ashcroft, Nature 2000)

Hydrogen: know and less know facts

- Solid hydrogen is insulating up to 3.5Mbars (DAC experiments, Loubeyre Nature '02)
- at T=0K molecular dissociation occurs at r_s=1.31 (DMC, Ceperley Alder PRB '87)
- At the molecular dissociation a diamond structure of protons is predicted. At higher pressure a diamond–bcc transition is expected (DMC, Natoli et al PRL '93).
- crystal structures of different symmetry can have very close energies: needs of very accurate total energy methods.
- Size effects are crucial to obtain accurate energies (Brillouin zone sampling in CPMD).
- ZPM is large and favors isotropic structures (Kitamura et al, Nature 2000).
- Molecular phases I and II are understood, phase III is still unsettled.
- Predicting metalization requires going beyond DFT-LDA-GGA (Johnson Ashcroft, Nature 2000)
- Most recent prediction (T=0K): $P_c \simeq$4Mbars within the molecular phase (DFT-Exact-Exchange functional) (Stadele and Martin, PRL 2000). But this method is too demanding to be used in a "dynamical" simulation.

Hydrogen: know and less know facts

- Solid hydrogen is insulating up to 3.5Mbars (DAC experiments, Loubeyre Nature '02)
- at T=0K molecular dissociation occurs at r_s=1.31 (DMC, Ceperley Alder PRB '87)
- At the molecular dissociation a diamond structure of protons is predicted. At higher pressure a diamond–bcc transition is expected (DMC, Natoli et al PRL '93).
- crystal structures of different symmetry can have very close energies: needs of very accurate total energy methods.
- Size effects are crucial to obtain accurate energies (Brillouin zone sampling in CPMD).
- ZPM is large and favors isotropic structures (Kitamura et al, Nature 2000).
- Molecular phases I and II are understood, phase III is still unsettled.
- Predicting metalization requires going beyond DFT-LDA-GGA (Johnson Ashcroft, Nature 2000)
- Most recent prediction (T=0K): $P_c \simeq$4Mbars within the molecular phase (DFT-Exact-Exchange functional) (Stadele and Martin, PRL 2000). But this method is too demanding to be used in a "dynamical" simulation.
- Molecular-atomic (insulating-metallic) transition in the liquid at higher temperature (T=1500K) has been recently predicted by CPMD (Scandolo, PNAS 2003) but not yet confirmed by experiments. At higher T ($\simeq$5000K) PIMC exhibits a continuous molecular-atomic transition.

CEIMC

CEIMC: Metropolis Monte Carlo for the finite T ions. The BO energy in the Boltzmann distribution is obtained by a QMC calculation for the gound state electrons.

- Finite temperature Ions: Noisy Monte Carlo The Penalty Method
- Ground state electrons:
  - VMC & RQMC
  - Moving the electrons: the bounce algorithm
  - Energy difference methods
  - Trial wave functions for hydrogen
  - Finite size effects: Twist Average Boundary Conditions (TABC) within CEIMC
- Pre-rejecting protonic moves: multilevel Metropolis
- Strategy for Protonic PIMC within CEIMC

Moving the ions

- In Metropolis MC we generate a Markov chain of ionic states S distributed according to Boltzmann

$$P(S) \propto \exp(-\beta E_{BO}(S))$$

$E_{BO}(S) =$ Born-Oppenheimer energy for the configuration S.

- Given an initial state S we propose a trial state S' with probability

$$T(S \rightarrow S') = T(S' \rightarrow S)$$

and we accept the move with probability

$$A(S \rightarrow S') = min\left[1, \exp\left\{-\beta[E_{BO}(S') - E_{BO}(S)]\right\}\right]$$

- After a finite number of moves the Markov chain is distributed with Boltzmann (if ergodicity holds).

- But $E_{BO}(S)$ from QMC is noisy $\Rightarrow$ use the penalty method

The Penalty Method

- Assume mean value and variance of the energy difference over the noise distribution exist

$$\begin{aligned} \beta[E_{BO}(S') - E_{BO}(S)] &= < \delta(S,S') >= \Delta(S,S') \\ < (\delta - \Delta)^2 > &= \sigma^2(S,S') \end{aligned}$$

We want to find the new acceptance probability $a(S \rightarrow S')$ such that we satisfy detailed balance on average:

$$T(S \rightarrow S') < a(S \rightarrow S') >= T(S' \rightarrow S) < a(S' \rightarrow S) > \exp[-\beta\Delta(S,S')]$$

where

$$< a(S \rightarrow S') >= \int_{-\infty}^{\infty} d\delta \underbrace{P(\delta|S,S')}_{\text{noise distribution}} a(\delta|S,S')$$

D.M.Ceperley and M.Dewing, J. Chem. Phys., **110**, 9812 (1999)

The Penalty Method

- Assume:

$$\begin{aligned} a(\delta|S,S') &= a(\delta) \\ P(\delta|S,S') &= P(-\delta|S',S) \end{aligned}$$

Detailed Balance is

$$\int_{-\infty}^{\infty} d\delta P(\delta|S,S') \left[a(\delta) - e^{-\Gamma} a(-\delta)\right] = 0 \qquad (1)$$

where

$$\Gamma(S \to S') = \Delta(S,S') - log\left[T(S' \to S)/T(S \to S')\right]$$

If $a(\delta)$ satisfies eq. (1), after a finite number of moves the Markov chain is distributed with Boltzmann (if ergodicity holds).

The Penalty Method

- Assume:

$$\begin{aligned} a(\delta|S,S') &= a(\delta) \\ P(\delta|S,S') &= P(-\delta|S',S) \end{aligned}$$

Detailed Balance is

$$\int_{-\infty}^{\infty} d\delta P(\delta|S,S') \left[a(\delta) - e^{-\Gamma} a(-\delta)\right] = 0 \qquad (0)$$

where

$$\Gamma(S \to S') = \Delta(S,S') - log\left[T(S' \to S)/T(S \to S')\right]$$

If $a(\delta)$ satisfies eq. (1), after a finite number of moves the Markov chain is distributed with Boltzmann (if ergodicity holds).

- If we assume $P(\delta|S,S')$ to be gaussian with known σ^2

$$P(\delta) = \frac{1}{\sqrt{2\pi\sigma^2}} \exp\left[\frac{-(\delta-\Delta)^2}{2\sigma^2}\right] \Longrightarrow a(\delta|\sigma) = min\left[1, \frac{T(S' \to S)}{T(S \to S')} \exp\left(-\delta - \frac{\sigma^2}{2}\right)\right]$$

The Penalty Method

- But noise must be extracted from the data:

$$\gamma = \frac{1}{M}\sum_k \delta_k \approx \Delta \qquad\qquad s^2 = \frac{1}{M-1}\left[\frac{1}{M}\sum_k (\delta_k - \gamma)^2\right] \approx \sigma^2$$

$$P(\delta) \rightarrow P(\gamma, s^2) = \underbrace{G(\gamma - \Delta, \sigma^2)}\ \underbrace{P_{n-1}(s^2, \sigma^2)}$$

normal distribution χ^2 distribution

Detailed balance is now a 2 parameter integral equation and the solution is a Bessel function. Using its asymptotic expansion one gets:

$$a(\gamma, s^2, M) = min\left[1, \frac{T(S' \rightarrow S)}{T(S \rightarrow S')} e^{-\left(\delta + \frac{s^2}{2} + \frac{s^4}{4(M+1)} + \frac{s^6}{3(M+1)(M+3)} + \cdots\right)}\right]$$

valid for $s^2 < 4M$ and very good for $s^2 < 0.1M$.

The Penalty Method

- But noise must be extracted from the data:

$$\gamma = \frac{1}{M}\sum_k \delta_k \approx \Delta \qquad\qquad s^2 = \frac{1}{M-1}\left[\frac{1}{M}\sum_k (\delta_k - \gamma)^2\right] \approx \sigma^2$$

$$P(\delta) \rightarrow P(\gamma, s^2) = \underbrace{G(\gamma - \Delta, \sigma^2)}\ \underbrace{P_{n-1}(s^2, \sigma^2)}$$

normal distribution $\qquad$ χ^2 distribution

Detailed balance is now a 2 parameter integral equation and the solution is a Bessel function. Using its asymptotic expansion one gets:

$$a(\gamma, s^2, M) = min\left[1, \frac{T(S' \rightarrow S)}{T(S \rightarrow S')} e^{-\left(\delta + \frac{s^2}{2} + \frac{s^4}{4(M+1)} + \frac{s^6}{3(M+1)(M+3)} + \cdots\right)}\right]$$

valid for $s^2 < 4M$ and very good for $s^2 < 0.1M$.

- **The noise always causes extra rejection !**

The Penalty Method

- EFFICIENCY: which level of noise is optimal?

  For a generic observable we ask which level of noise minimizes its statistical error ϵ^2 at fixed computer time T: $T = m[nt + t_0]$

  m=total number of ionic steps attempted

  n=number of electronic calculations before the acceptance test

  t=CPU time for a single electronic calculation

  t_0=time in the noiseless part of the code per total step

  In general $\epsilon = c(s)m^{-(1/2)}$ and $s = dn^{-(1/2)}$. ($c(s)$ and d are unknown).

  A measure of the inefficiency of our calculation is:

$$T\epsilon^2 = c^2(s)t_0\left[1 + \frac{f}{s^2}\right] \qquad\qquad f = d^2\frac{t}{t_0}$$

  For any given application we have to chose s which minimize this quantity.

The Penalty Method

- EFFICIENCY: which level of noise is optimal?
  For a generic observable we ask which level of noise minimizes its statistical error ϵ^2 at fixed computer time T: $T = m[nt + t_0]$
  m=total number of ionic steps attempted
  n=number of electronic calculations before the acceptance test
  t=CPU time for a single electronic calculation
  t_0=time in the noiseless part of the code per total step
  In general $\epsilon = c(s)m^{-(1/2)}$ and $s = dn^{-(1/2)}$. ($c(s)$ and d are unknown).
  A measure of the inefficiency of our calculation is:

$$T\epsilon^2 = c^2(s)t_0\left[1 + \frac{f}{s^2}\right] \qquad\qquad f = d^2\frac{t}{t_0}$$

  For any given application we have to chose s which minimize this quantity.

- In few simple examples the optimal noise level was found to be $s^2 \approx 1$.
  In CEIMC other constraints imposes the noise level but as a rule of thumb we always try to stay around 1.

The electronic problem

System of N_p ions and N_e electrons. We need to compute the BO energy

$$E_{BO}(S) = < \Phi_0(S)|\hat{H}|\Phi_0(S) >$$

$|\Phi_0(S) >=$ electronic ground state w.f. for ionic state $S = \{\vec{s}_1, \ldots, \vec{s}_{N_p}\}$.
In configurational space $X = (R, \Sigma) = (\{r_1, \ldots, r_{N_e}\}, \{\sigma_1, \ldots, \sigma_{N_e}\})$

$$E_{BO}(S) = \int dX \, |\Phi_0(X|S)|^2 \, E_L(X|S); \qquad E_L(X|S) = \frac{\hat{H}(R,S)\Phi_0(X|S)}{\Phi_0(X|S)}$$

$$\sigma^2(S) = \int dX \, |\Phi_0(X|S)|^2 \, [(E_L(X|S) - E_{BO}(S)]^2$$

The electronic problem

System of N_p ions and N_e electrons. We need to compute the BO energy

$$E_{BO}(S) = < \Phi_0(S)|\hat{H}|\Phi_0(S) >$$

$|\Phi_0(S) >=$ electronic ground state w.f. for ionic state $S = \{\vec{s}_1, \ldots, \vec{s}_{N_p}\}$.
In configurational space $X = (R, \Sigma) = (\{r_1, \ldots, r_{N_e}\}, \{\sigma_1, \ldots, \sigma_{N_e}\})$

$$E_{BO}(S) = \int dX \, |\Phi_0(X|S)|^2 \, E_L(X|S); \qquad E_L(X|S) = \frac{\hat{H}(R,S)\Phi_0(X|S)}{\Phi_0(X|S)}$$

$$\sigma^2(S) = \int dX \, |\Phi_0(X|S)|^2 \, [(E_L(X|S) - E_{BO}(S)]^2$$

- If $|\Phi_0(S) >$ is an eigenfunction of $\hat{H}$

$$\begin{cases} E_L(X|S) & = E_{BO}(S) \\ \sigma^2(S) & = 0 \end{cases}$$

zero variance principle

Variational Monte Carlo - VMC 1

- The "Variational Theorem": assume a trial wave function for the electrons in the external field of the ions $\Psi_T(X|S)$ and compute the total energy as the average of the local energy $E_L = \Psi_T^{-1} H \Psi_T$

$$E_0 \leq E_T = \frac{< \Psi_T | \hat{H} | \Psi_T >}{< \Psi_T | \Psi_T >} = \frac{\int dX |\Psi_T(X;S)|^2 \Psi_T^{-1}(X;S) \hat{H} \Psi_T(X;S)}{\int dX |\Psi_T(X;S)|^2}$$

Variational Monte Carlo - VMC 1

- The "Variational Theorem": assume a trial wave function for the electrons in the external field of the ions $\Psi_T(X|S)$ and compute the total energy as the average of the local energy $E_L = \Psi_T^{-1} H \Psi_T$

$$E_0 \leq E_T = \frac{< \Psi_T | \hat{H} | \Psi_T >}{< \Psi_T | \Psi_T >} = \frac{\int dX |\Psi_T(X;S)|^2 \Psi_T^{-1}(X;S) \hat{H} \Psi_T(X;S)}{\int dX |\Psi_T(X;S)|^2}$$

- The functional form of the trial wave function must be suitable
  - continuous
  - of proper symmetry
  - normalizable
  - with finite variance (for MC only)

Variational Monte Carlo - VMC 1

- The "Variational Theorem": assume a trial wave function for the electrons in the external field of the ions $\Psi_T(X|S)$ and compute the total energy as the average of the local energy $E_L = \Psi_T^{-1} H \Psi_T$

$$E_0 \leq E_T = \frac{< \Psi_T | \hat{H} | \Psi_T >}{< \Psi_T | \Psi_T >} = \frac{\int dX |\Psi_T(X;S)|^2 \Psi_T^{-1}(X;S) \hat{H} \Psi_T(X;S)}{\int dX |\Psi_T(X;S)|^2}$$

- The functional form of the trial wave function must be suitable
  - continuous
  - of proper symmetry
  - normalizable
  - with finite variance (for MC only)
- Parametrized: for a given functional form Ψ_T depends on a number of parameters $\vec{\alpha} = (\alpha_1, \ldots, \alpha_n)$

$$\Psi_T(X|S,\vec{\alpha}) \Longrightarrow E_T(S,\vec{\alpha}) = \langle E_L(X|S,\vec{\alpha}) \rangle$$

VMC 2

1. Since $|\Psi_T|^2 \geq 0$ use Metropolis MC to sample $P(X|S,\alpha) = |\Psi_T|^2 / \int dr |\Psi_T|^2$.
2. take averages of the local energy and the variance
3. optimize over $\{\alpha_i\}$ by minimizing energy and/or variance
4. repeat until convergence is reached

VMC 3

- advantages:
  - VMC can use any computable and suitable trial function
  - easy to implement and very robust
  - learn directly what works in wave functions
  - no sign problem for fermions!

VMC 3

- advantages:
  - VMC can use any computable and suitable trial function
  - easy to implement and very robust
  - learn directly what works in wave functions
  - no sign problem for fermions!
- problems:
  - favors simple states over more complicated states (e.g. solid is more accurate than liquid)
  - the optimization is time consuming (human and machine). It introduces an element of human bias in the calculation.
  - variational energy is quite insensitive to long range order. Error in the energy and variance are second order in the trial function while for other properties (like correlation functions) it is first order.

VMC 3

- advantages:
  - VMC can use any computable and suitable trial function
  - easy to implement and very robust
  - learn directly what works in wave functions
  - no sign problem for fermions!
- problems:
  - favors simple states over more complicated states (e.g. solid is more accurate than liquid)
  - the optimization is time consuming (human and machine). It introduces an element of human bias in the calculation.
  - variational energy is quite insensitive to long range order. Error in the energy and variance are second order in the trial function while for other properties (like correlation functions) it is first order.
- an automatic optimization method is preferable

Projection Monte Carlo

Project $|\Psi_T>$ onto the true ground state $|\Phi_0>$ by applying some projection operator $\hat{P}$.

- Diffusion MC (DMC) and Reptation Quantum MC (RQMC) / (VPI) : $\hat{P} = e^{-t\hat{H}}$
- Green Function MC (GFMC) : $\hat{P} = [\hat{1} + t\hat{H}]^{-1}$
- Power MC : $\hat{P} = \hat{1} - t\hat{H}$ (lattice models)

RQMC - 1

$|\Psi_T> = \sum_i c_i \ |\Phi_i>$ ⟵ eigenstates of $\hat{H}$

RQMC - 1

$$|\Psi_T>=\sum_i c_i \ |\Phi_i> \longleftarrow \text{eigenstates of } \hat{H}$$

$$|\Psi(t)>\equiv e^{-t\hat{H}}|\Psi_T>=\sum_i c_i e^{-tE_i}|\Phi_i>\Longrightarrow \lim_{t\to\infty}|\Psi(t)>\propto |\Phi_0>$$

RQMC - 1

$$|\Psi_T>=\sum_i c_i \ |\Phi_i> \longleftarrow \text{eigenstates of } \hat{H}$$

$$|\Psi(t)>\equiv e^{-t\hat{H}}|\Psi_T>=\sum_i c_i e^{-tE_i}|\Phi_i>\Longrightarrow \lim_{t\to\infty}|\Psi(t)>\propto |\Phi_0>$$

$$E(t)=\frac{<\Psi(t/2)|\hat{H}|\Psi(t/2)>}{<\Psi(t/2)|\Psi(t/2)>}=\frac{<\Psi_T|e^{-\frac{t}{2}\hat{H}}\hat{H}e^{-\frac{t}{2}\hat{H}}|\Psi_T>}{<\Psi_T|e^{-t\hat{H}}|\Psi_T>}$$

RQMC - 1

$$|\Psi_T>=\sum_i c_i \ |\Phi_i> \longleftarrow \text{eigenstates of } \hat{H}$$

$$|\Psi(t)>\equiv e^{-t\hat{H}}|\Psi_T>=\sum_i c_i e^{-tE_i}|\Phi_i>\Longrightarrow \lim_{t\to\infty}|\Psi(t)>\propto |\Phi_0>$$

$$E(t)=\frac{<\Psi(t/2)|\hat{H}|\Psi(t/2)>}{<\Psi(t/2)|\Psi(t/2)>}=\frac{<\Psi_T|e^{-\frac{t}{2}\hat{H}}\hat{H}e^{-\frac{t}{2}\hat{H}}|\Psi_T>}{<\Psi_T|e^{-t\hat{H}}|\Psi_T>}$$

Define the generating function of the moments

$$Z(t)=<\Psi_T|e^{-t\hat{H}}|\Psi_T>\Longrightarrow\begin{cases}E(t)=-\partial_t\log Z(t)=<E_L>_t & \longrightarrow E_0\\ & t\to\infty\\ \sigma^2(t)=\partial_t^2\log Z(t)=-\partial_t E(t)>0 & \longrightarrow 0\end{cases}$$

RQMC - 1

$$|\Psi_T>=\sum_i c_i \ |\Phi_i> \longleftarrow \text{eigenstates of } \hat{H}$$

$$|\Psi(t)>\equiv e^{-t\hat{H}}|\Psi_T>=\sum_i c_i e^{-tE_i}|\Phi_i>\Longrightarrow \lim_{t\to\infty}|\Psi(t)>\propto |\Phi_0>$$

$$E(t)=\frac{<\Psi(t/2)|\hat{H}|\Psi(t/2)>}{<\Psi(t/2)|\Psi(t/2)>}=\frac{<\Psi_T|e^{-\frac{t}{2}\hat{H}}\hat{H}e^{-\frac{t}{2}\hat{H}}|\Psi_T>}{<\Psi_T|e^{-t\hat{H}}|\Psi_T>}$$

Define the generating function of the moments

$$Z(t)=<\Psi_T|e^{-t\hat{H}}|\Psi_T>\Longrightarrow\begin{cases}E(t)=-\partial_t\log Z(t)=<E_L>_t & \longrightarrow E_0\\ & t\to\infty\\ \sigma^2(t)=\partial_t^2\log Z(t)=-\partial_t E(t)>0 & \longrightarrow 0\end{cases}$$

- The energy converges monotonously from above ($\partial_t E(t)\leqslant 0$)

RQMC - 1

$$|\Psi_T>=\sum_i c_i \ |\Phi_i> \longleftarrow \text{eigenstates of } \hat{H}$$

$$|\Psi(t)>\equiv e^{-t\hat{H}}|\Psi_T>=\sum_i c_i e^{-tE_i}|\Phi_i>\Longrightarrow \lim_{t\to\infty}|\Psi(t)>\propto |\Phi_0>$$

$$E(t)=\frac{<\Psi(t/2)|\hat{H}|\Psi(t/2)>}{<\Psi(t/2)|\Psi(t/2)>}=\frac{<\Psi_T|e^{-\frac{t}{2}\hat{H}}\hat{H}e^{-\frac{t}{2}\hat{H}}|\Psi_T>}{<\Psi_T|e^{-t\hat{H}}|\Psi_T>}$$

Define the generating function of the moments

$$Z(t)=<\Psi_T|e^{-t\hat{H}}|\Psi_T>\Longrightarrow\begin{cases}E(t)=-\partial_t\log Z(t)=<E_L>_t & \longrightarrow E_0\\ & t\to\infty\\ \sigma^2(t)=\partial_t^2\log Z(t)=-\partial_t E(t)>0 & \longrightarrow 0\end{cases}$$

- The energy converges monotonously from above ($\partial_t E(t)\leqslant 0$)

- At any finite time t, $E(t)$ is a variational upper bound to E_0: $E(t)\geqslant E_0$

RQMC - 2

In configuration space

$$Z(t) = \int dR dR' < \Psi_T | R > \rho(R, R', t) < R' | \Psi_T >$$

$\rho(R, R', t) =< R|e^{-t\hat{H}}|R' >$ is the thermal density matrix at inverse temperature t.

RQMC - 2

In configuration space

$$Z(t) = \int dR dR' < \Psi_T | R > \rho(R, R', t) < R' | \Psi_T >$$

$\rho(R, R', t) =< R|e^{-t\hat{H}}|R' >$ is the thermal density matrix at inverse temperature t.

1 - Factorization ($t = M\tau$)

$$\rho(R, R', t) =< R|(e^{-\tau\hat{H}})^M|R' >= \int dR_1 \cdots dR_{M-1} \prod_{k=1}^{M-1} \rho(R_{k-1}, R_k, \tau)$$

$R_0 = R, R_M = R'$ paths boundary conditions in imaginary time

RQMC - 2

In configuration space

$$Z(t) = \int dR dR' < \Psi_T | R > \rho(R, R', t) < R' | \Psi_T >$$

$\rho(R, R', t) =< R|e^{-t\hat{H}}|R' >$ is the thermal density matrix at inverse temperature t.

1 - Factorization ($t = M\tau$)

$$\rho(R, R', t) =< R|(e^{-\tau\hat{H}})^M|R' >= \int dR_1 \cdots dR_{M-1} \prod_{k=1}^{M-1} \rho(R_{k-1}, R_k, \tau)$$

$R_0 = R, R_M = R'$ paths boundary conditions in imaginary time

2 - Importance Sampling break-up: $\hat{H} = \hat{\mathcal{H}} + E_L(R)$

$$\begin{aligned} \hat{\mathcal{H}} &= \lambda \left[-\nabla^2 + \frac{\nabla^2 \Psi_T}{\Psi_T} \right] \\ E_L(R) &= V(R) - \lambda \frac{\nabla^2 \Psi_T}{\Psi_T} \end{aligned}$$

RQMC - 3

$$\rho(R_{k-1},R_k,\tau) \simeq < R_{k-1}|e^{-\tau\hat{\mathcal{H}}}|R_k >^s e^{-\frac{\tau}{2}\left[E_L(R_k)+E_L(R_{k-1})\right]}$$

$$< R_{k-1}|e^{-\tau\hat{\mathcal{H}}}|R_k >^s = (4\pi\lambda\tau)^{-\frac{3N}{2}}\, e^{-L_s(R_{k-1},R_k,\tau)}$$

$$L_s(R_{k-1},R_k,\tau) = \frac{(R_k-R_{k-1})^2}{4\lambda\tau} + \frac{\lambda\tau}{2}(F_k^2+F_{k-1}^2) + \frac{(R_k-R_{k-1})\cdot(F_k-F_{k-1})}{2}$$

Putting all pieces together

$$\rho(R,R',t) = \int \prod_{k=1}^{M-1} dR_k \left[\prod_{k=1}^{M} \frac{e^{-L_s(R_{k-1},R_k,\tau)}}{(4\pi\lambda\tau)^{3N/2}}\right] e^{-\tau\left[\frac{E_L(R_0)}{2}+\sum_{k=1}^{M-1} E_L(R_k)+\frac{E_L(R_M)}{2}\right]}$$

$$Z(t) = \int dR dR' < \Psi_T|R > \rho(R,R',t) < R'|\Psi_T >$$

Summary of FN-RQMC

- Build a path $Q = (R_0, \ldots, R_M)$ for the system of N_e electrons at fixed ionic configuration S.
- Sample the path space according to the distribution

$$\begin{aligned}
\mathbf{\Pi(Q|S)} &= \exp\left[- U(R_0|S) - U(R_M|S) - A(Q|S)\right] \\
U(R|S) &= \Re[\ln \Psi_T(R|S)] \\
A(Q|S) &= \sum_{k=1}^{M} L_s(R_{k-1}, R_k, \tau|S) + \tau \left[\frac{E_L(R_0|S)}{2} + \sum_{k=1}^{M-1} E_L(R_k|S) + \frac{E_L(R_M|S)}{2} \right]
\end{aligned}$$

- **FN:** check $\Psi_T(R_{k-1})\Psi_T(R_k) > 0$ along the path. Otherwise reject the new path.
- Compute the local energy and the variance at path ends, other properties at the middle:

$$O(t) = \frac{1}{Z(t)} \int dR_1 dR_2 dR_3 \Psi_T^*(R_1) \rho(R_1, R_2|\frac{t}{2}) < R_2|\hat{O}|R_2 > \rho(R_2, R_3|\frac{t}{2}) \Psi_T(R_3)$$

no mixed estimators bias!!!

- ensure convergence to the continuum limit ($\tau \to 0$) and to the ground state ($t \to \infty$)

Sampling the electrons

VMC: with backflow wave functions we need to performe global moves.

Sampling the electrons

VMC: with backflow wave functions we need to performe global moves.

RQMC: classical algorithm

- One end of the *many-body polymer* is sampled with probability 1/2 to be the growth end R_g

$$d = \begin{cases} +1 & \Rightarrow R_g = R_M \\ -1 & \Rightarrow R_g = R_0 \end{cases}$$

- A link is added to the growth end and removed from the opposite end in order to keep the polymer length constant. The transition probability is factorized as

$$P_d(Q \rightarrow Q') = T_d(Q \rightarrow Q') a_d(Q \rightarrow Q')$$

The choice

$$a_d(Q \rightarrow Q') = min\left[1, \frac{\Pi(Q') T_{-d}(Q' \rightarrow Q)}{\Pi(Q) T_d(Q \rightarrow Q')}\right]$$

ensures the detailed balance

$$\Pi(Q) P_d(Q \rightarrow Q') = \Pi(Q') P_{-d}(Q' \rightarrow Q)$$

Sampling the electrons

VMC: with backflow wave functions we need to performe global moves.

RQMC: classical algorithm

- One end of the *many-body polymer* is sampled with probability 1/2 to be the growth end R_g

$$d = \begin{cases} +1 & \Rightarrow R_g = R_M \\ -1 & \Rightarrow R_g = R_0 \end{cases}$$

- A link is added to the growth end and removed from the opposite end in order to keep the polymer length constant. The transition probability is factorized as

$$P_d(Q \rightarrow Q') = T_d(Q \rightarrow Q') a_d(Q \rightarrow Q')$$

The choice

$$a_d(Q \rightarrow Q') = min\left[1, \frac{\Pi(Q') T_{-d}(Q' \rightarrow Q)}{\Pi(Q) T_d(Q \rightarrow Q')}\right]$$

ensures the detailed balance

$$\Pi(Q) P_d(Q \rightarrow Q') = \Pi(Q') P_{-d}(Q' \rightarrow Q)$$

Problems: a) the memory of this algorithm in MC step scales as $(\#beads)^2$/acceptance.

b) persistent configurations can appear

The bounce algorithm

Bounce algorithm: choose at random one end of the chain at the beginning of the Markov chain and reverse the growth direction upon rejection only. Minimal modification of the algorithm and solve both problems

Proof of the Bounce algorithm:

- enlarge the configurational space $\{Q, d\}$ and define $P(Q, d \to Q', d')$.
- assuming ergodicity, the Markov chain converges to a unique stationary state, $\Upsilon(Q, d)$ solution of the eigenvalue equation:

$$\sum_{Q,d} \Upsilon(Q, d)\, P(Q, d \to Q', d') = \Upsilon(Q', d').$$

- allowed transitions

$$P(Q, d \to Q', d') \neq 0 \Longleftrightarrow \begin{cases} d = d' & , Q \neq Q' \quad \text{accepted move} \\ d' = -d & , Q = Q' \quad \text{rejected move.} \end{cases}$$

- assume $d' = +1$. Since $\Pi(Q)$ does not depend on d

$$\Pi(Q')P(Q', -1 \to Q', 1) + \sum_{Q \neq Q'} \Pi(Q)P(Q, 1 \to Q', 1) = \Pi(Q').$$

The bounce algorithm

- DB $(\Pi(Q)P(Q,1 \to Q',1) = \Pi(Q')P(Q',-1 \to Q,-1))$ provides

$$\Pi(Q')\left[P(Q',-1 \to Q',1) + \sum_{Q} P(Q',-1 \to Q,-1)\right] = \Pi(Q')$$

The term in the bracket exhausts all possibilities for a move from the state $(Q',-1)$, thus it adds to one. Hence $\Pi(Q)$ is a solution and by the theory of Markov chains, it is the unique probability distribution of the stationary state.

The bounce algorithm

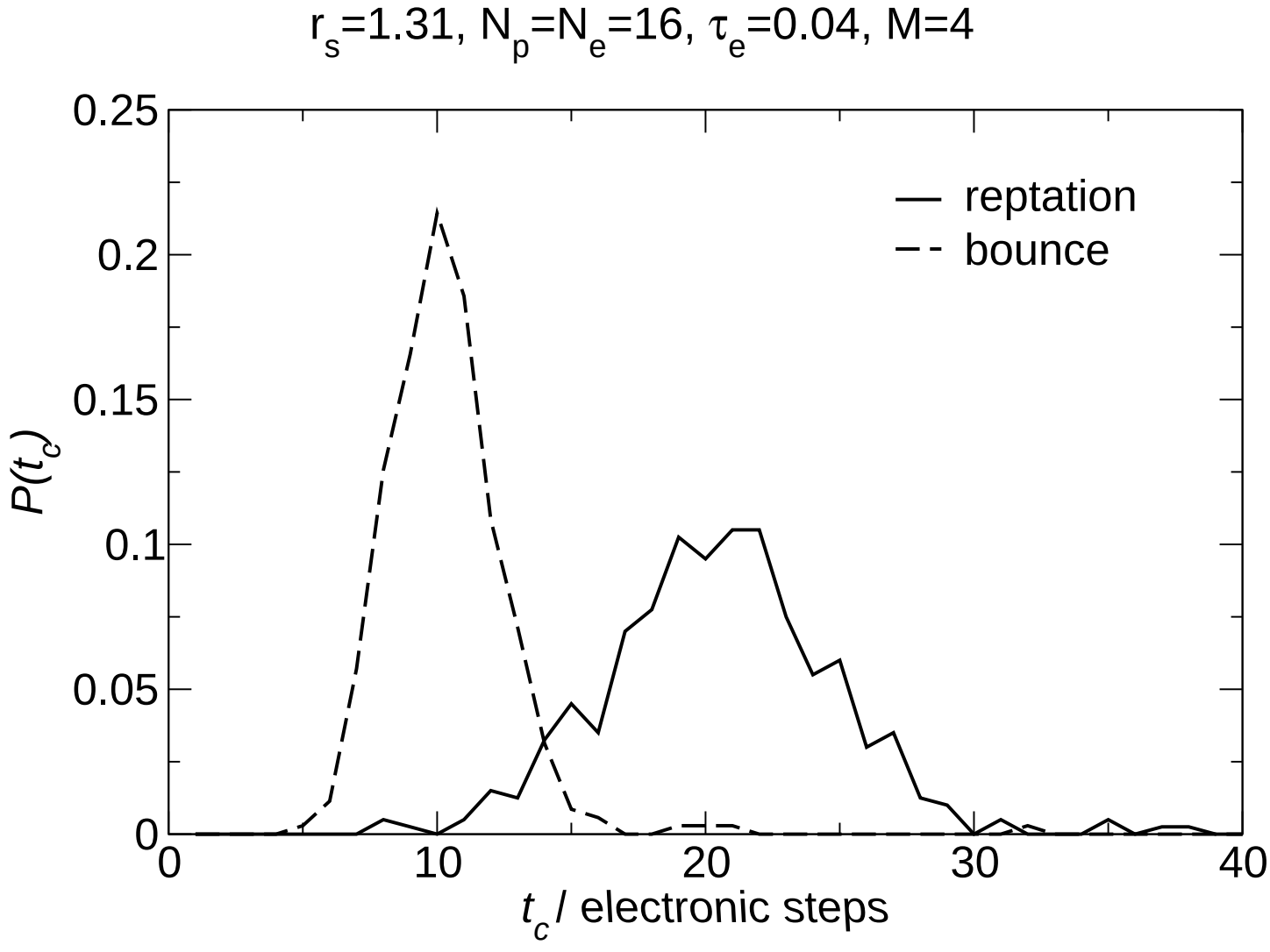

Probability distribution of the correlation time of the energy difference between two fixed protonic configurations (S, S').

The bounce algorithm

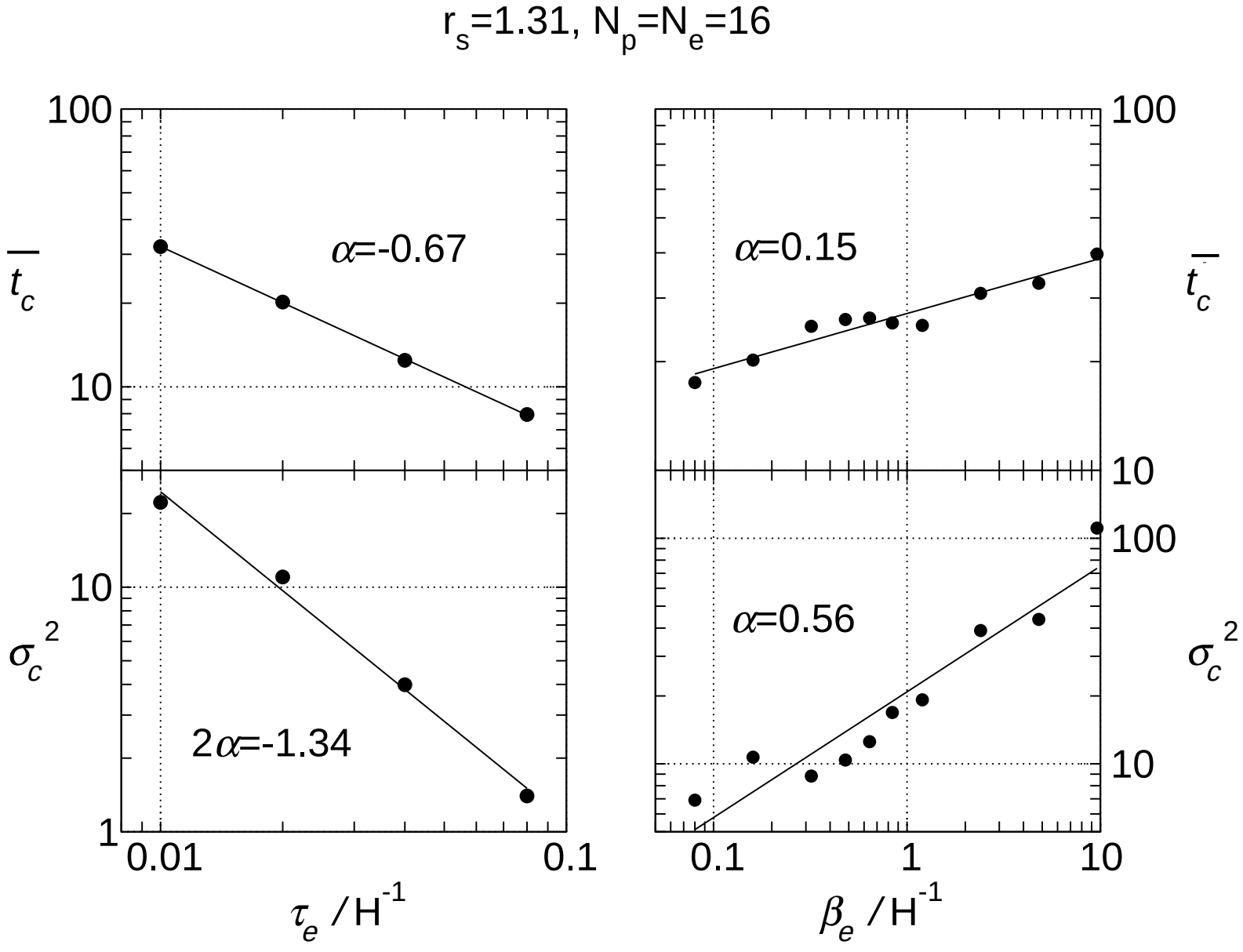

Energy difference method

- In CEIMC we need to evaluate the energy difference between two closeby protonic configurations (S,S').

Energy difference method

- In CEIMC we need to evaluate the energy difference between two closeby protonic configurations (S,S').
- Two independent electronic calculations (uncorrelated sampling) is very inefficient for $\Delta E << E$.

Energy difference method

- In CEIMC we need to evaluate the energy difference between two closeby protonic configurations (S,S').
- Two independent electronic calculations (uncorrelated sampling) is very inefficient for $\Delta E << E$.
- Optimal sampling function: minimizes the variance of the energy difference

$$P(Q|S,S') \propto \left|\Pi(Q|S)(E_S - < E_S >) - \Pi(Q|S')(E_{S'} - < E_{S'} >)\right|$$

but it requires an estimate of $< E_S >, < E_{S'} >$.

Energy difference method

- In CEIMC we need to evaluate the energy difference between two closeby protonic configurations (S,S').
- Two independent electronic calculations (uncorrelated sampling) is very inefficient for $\Delta E << E$.
- Optimal sampling function: minimizes the variance of the energy difference

$$P(Q|S,S') \propto \left|\Pi(Q|S)(E_S - < E_S >) - \Pi(Q|S')(E_{S'} - < E_{S'} >)\right|$$

  but it requires an estimate of $< E_S >, < E_{S'} >$.
- simpler form: $P(Q|S,S') \propto \Pi(Q|S) + \Pi(Q|S')$

Energy difference method

- In CEIMC we need to evaluate the energy difference between two closeby protonic configurations (S,S').
- Two independent electronic calculations (uncorrelated sampling) is very inefficient for $\Delta E << E$.
- Optimal sampling function: minimizes the variance of the energy difference

$$P(Q|S,S') \propto \left|\Pi(Q|S)(E_S - < E_S >) - \Pi(Q|S')(E_{S'} - < E_{S'} >)\right|$$

  but it requires an estimate of $< E_S >, < E_{S'} >$.
- simpler form: $P(Q|S,S') \propto \Pi(Q|S) + \Pi(Q|S')$
- These two forms have the properties that
  - sample regions of both configuration spaces (S and S')
  - make the energy difference bounded

Energy difference method

- In CEIMC we need to evaluate the energy difference between two closeby protonic configurations (S,S').
- Two independent electronic calculations (uncorrelated sampling) is very inefficient for $\Delta E << E$.
- Optimal sampling function: minimizes the variance of the energy difference

$$P(Q|S,S') \propto \left|\Pi(Q|S)(E_S - < E_S >) - \Pi(Q|S')(E_{S'} - < E_{S'} >)\right|$$

  but it requires an estimate of $< E_S >, < E_{S'} >$.
- simpler form: $P(Q|S,S') \propto \Pi(Q|S) + \Pi(Q|S')$
- These two forms have the properties that
  - sample regions of both configuration spaces (S and S')
  - make the energy difference bounded
- compute properties for the system S by reweighting technique (RQMC easier than DMC).

Energy difference method

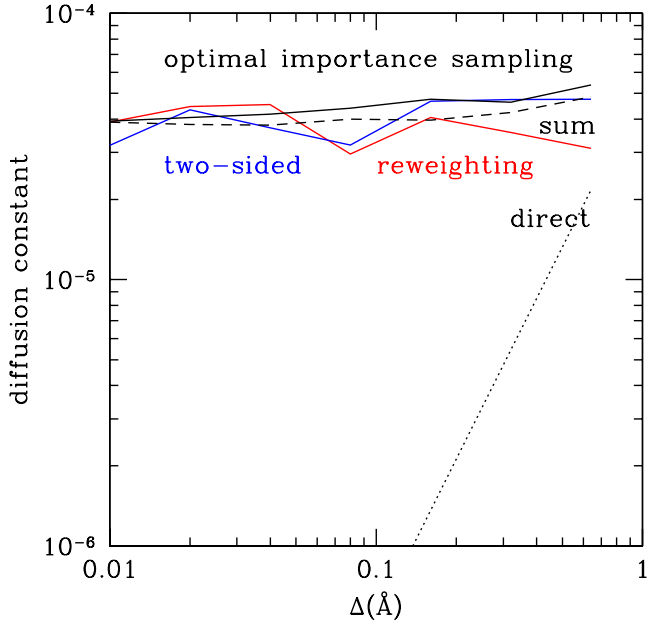

Efficiency versus importance function on a system with $N_e = N_p = 16$ and $r_s = 1.31$. In one system the protons are taken in a simple cubic lattice and in the other they are displaced randomly, with an average displacement of Δ. The diffusion constant is defined as Δ^2/T_{CPU} where T_{CPU} is the computer time needed to calculate the energy difference to an accuracy of $1000\ K$.

Finite size effects: TABC

- In the metallic systems finite size effects coming from the discrete structure of the Fermi surface are dominant and must be carefully treated.
  The finite size effects can be reduced to the classical $1/N$ behavior averaging over the undetermined phase of the wave function (Li et al. PRE 2001). For periodic systems we have

$$\Psi(\vec{r}_1 + L\hat{\vec{x}}, \vec{r}_2, \cdots) = e^{i\theta_x}\Psi(\vec{r}_1, \vec{r}_2, \cdots) \qquad \theta \in [-\pi, \pi)$$

  TABC:

$$A = \frac{1}{(2\pi)^3}\int_{-\pi}^{\pi} d^3\theta < \Psi_\theta|A|\Psi_\theta >$$

Finite size effects: TABC

- In the metallic systems finite size effects coming from the discrete structure of the Fermi surface are dominant and must be carefully treated.
  The finite size effects can be reduced to the classical $1/N$ behavior averaging over the undetermined phase of the wave function (Li et al. PRE 2001). For periodic systems we have

$$\Psi(\vec{r}_1 + L\hat{\vec{x}}, \vec{r}_2, \cdots) = e^{i\theta_x}\Psi(\vec{r}_1, \vec{r}_2, \cdots) \qquad \theta \in [-\pi, \pi)$$

  TABC:

$$A = \frac{1}{(2\pi)^3}\int_{-\pi}^{\pi} d^3\theta < \Psi_\theta|A|\Psi_\theta >$$

- In practice θ can be chosen on a 3D grid and independent calculations be performed for each grid point.

Finite size effects: TABC

- In the metallic systems finite size effects coming from the discrete structure of the Fermi surface are dominant and must be carefully treated.
  The finite size effects can be reduced to the classical $1/N$ behavior averaging over the undetermined phase of the wave function (Li et al. PRE 2001). For periodic systems we have

$$\Psi(\vec{r}_1 + L\hat{\vec{x}}, \vec{r}_2, \cdots) = e^{i\theta_x}\Psi(\vec{r}_1, \vec{r}_2, \cdots) \qquad \theta \in [-\pi, \pi)$$

  TABC:

$$A = \frac{1}{(2\pi)^3}\int_{-\pi}^{\pi} d^3\theta < \Psi_\theta|A|\Psi_\theta >$$

- In practice θ can be chosen on a 3D grid and independent calculations be performed for each grid point.
- or one can sample the twist angle at random and run different calculations.

Finite size effects: TABC

- In the metallic systems finite size effects coming from the discrete structure of the Fermi surface are dominant and must be carefully treated.
  The finite size effects can be reduced to the classical $1/N$ behavior averaging over the undetermined phase of the wave function (Li et al. PRE 2001). For periodic systems we have

$$\Psi(\vec{r}_1 + L\hat{\vec{x}}, \vec{r}_2, \cdots) = e^{i\theta_x}\Psi(\vec{r}_1, \vec{r}_2, \cdots) \qquad \theta \in [-\pi, \pi)$$

  TABC:

$$A = \frac{1}{(2\pi)^3}\int_{-\pi}^{\pi} d^3\theta < \Psi_\theta|A|\Psi_\theta >$$

- In practice θ can be chosen on a 3D grid and independent calculations be performed for each grid point.
- or one can sample the twist angle at random and run different calculations.
- No extra cost for TABC in CEIMC since we sum over twist angles to reduce the noise.

Finite size effects: TABC

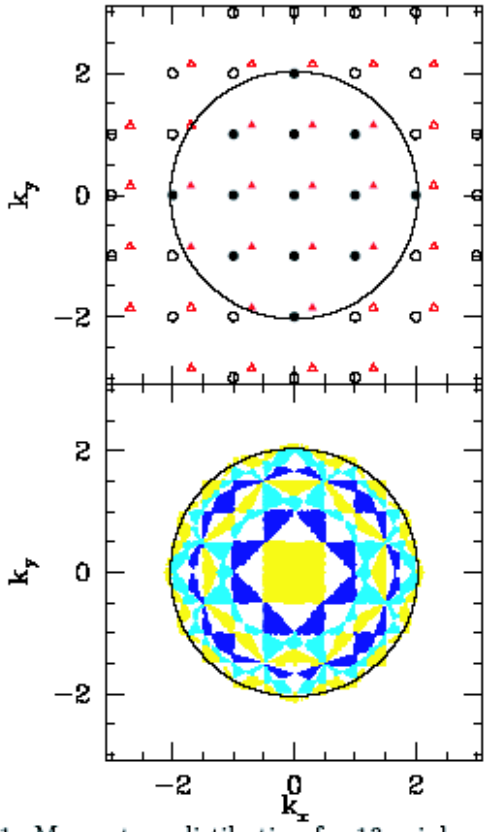

FIG. 1. Momentum distibution for 13 spinless fermions in a 2D square with side $L = 2\pi$. The top panel shows the occupied states (closed symbols) and empty states (open symbols) with zero twist (circles, PBC) and a twist equal to $2\pi(0.3, 0.15)$ (triangles). The circle shows the infinite system fermi surface. The bottom panel shows the occupied states with TABC. The colored regions show the occupied region for the lowest level (middle square), the third level, up to the outermost 13^{th} level.

Lin, Zong, Ceperley PRE 64, 016702 (2001)

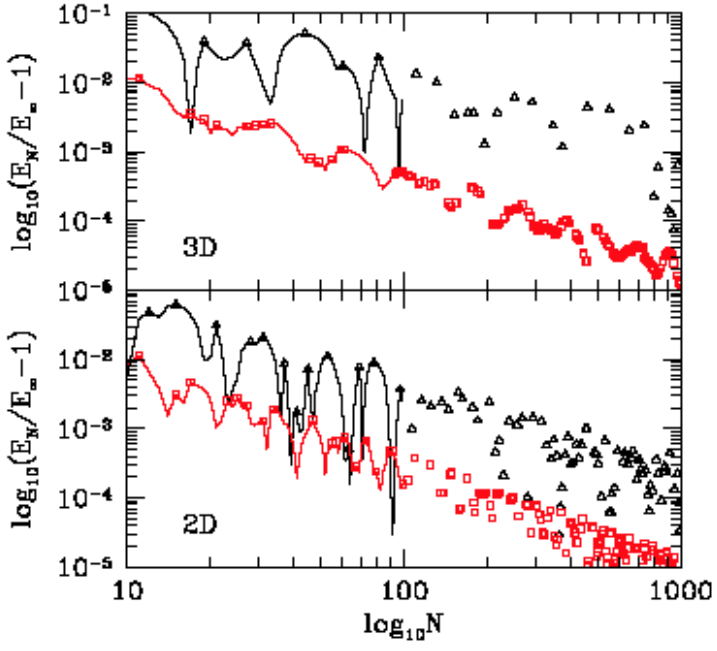

FIG. 2. Relative error of the energy versus number of particles with PBC (△) and TABC (□) in 2D and 3D. The points shown are only those where the relative error has a local maximum. Curves are shown only for $N < 100$.

Trial wave functions: $|\Psi_T>$

- Slater-Jastrow form

$$\Psi_T(R|S) = \exp\left[-U(R|S)\right] \mathrm{Det}\left(\Sigma^{\uparrow}\right) \mathrm{Det}\left(\Sigma^{\downarrow}\right)$$

Trial wave functions: $|\Psi_T>$

- Slater-Jastrow form

$$\Psi_T(R|S) = \exp\left[-U(R|S)\right] \mathrm{Det}\left(\Sigma^{\uparrow}\right) \mathrm{Det}\left(\Sigma^{\downarrow}\right)$$

- $U(R)$ is a (two-body + three-body + . . .) correlation factor (”pseudopotential”)

Trial wave functions: $|\Psi_T>$

- Slater-Jastrow form

$$\Psi_T(R|S) = \exp\left[-U(R|S)\right] \mathrm{Det}\left(\Sigma^{\uparrow}\right) \mathrm{Det}\left(\Sigma^{\downarrow}\right)$$

- $U(R)$ is a (two-body + three-body + . . .) correlation factor (”pseudopotential”)
- $\Sigma^{\uparrow}$ is a Slater determinant of single electron orbitals $\theta_k(\vec{x}_i, \sigma_i|S)$.

Trial wave functions: $|\Psi_T>$

- Slater-Jastrow form

$$\Psi_T(R|S) = \exp\left[-U(R|S)\right] \mathrm{Det}\left(\Sigma^{\uparrow}\right) \mathrm{Det}\left(\Sigma^{\downarrow}\right)$$

- $U(R)$ is a (two-body + three-body + . . .) correlation factor (”pseudopotential”)
- $\Sigma^{\uparrow}$ is a Slater determinant of single electron orbitals $\theta_k(\vec{x}_i, \sigma_i|S)$.
- The nodes are determined by the form of the orbitals only. They are the most important part of the trial function since the nodes are not optimized by projection.

Trial wave functions: $|\Psi_T>$

- Slater-Jastrow form

$$\Psi_T(R|S) = \exp\left[-U(R|S)\right] \mathrm{Det}\left(\Sigma^{\uparrow}\right) \mathrm{Det}\left(\Sigma^{\downarrow}\right)$$

- $U(R)$ is a (two-body + three-body + . . .) correlation factor ("pseudopotential")
- $\Sigma^{\uparrow}$ is a Slater determinant of single electron orbitals $\theta_k(\vec{x}_i, \sigma_i|S)$.
- The nodes are determined by the form of the orbitals only. They are the most important part of the trial function since the nodes are not optimized by projection.
  Dense hydrogen
  - metallic state: plane waves in terms of bare or dressed coordinates (backflow)

Trial wave functions: $|\Psi_T>$

- Slater-Jastrow form

$$\Psi_T(R|S) = \exp\left[-U(R|S)\right] \mathrm{Det}\left(\Sigma^{\uparrow}\right) \mathrm{Det}\left(\Sigma^{\downarrow}\right)$$

- $U(R)$ is a (two-body + three-body + . . .) correlation factor ("pseudopotential")
- $\Sigma^{\uparrow}$ is a Slater determinant of single electron orbitals $\theta_k(\vec{x}_i, \sigma_i|S)$.
- The nodes are determined by the form of the orbitals only. They are the most important part of the trial function since the nodes are not optimized by projection.
  Dense hydrogen
  - metallic state: plane waves in terms of bare or dressed coordinates (backflow)
  - molecular state: molecular orbitals (LCAO or any other reasonable form)

Trial wave functions: $|\Psi_T>$

- Slater-Jastrow form

$$\Psi_T(R|S) = \exp\left[-U(R|S)\right] \mathrm{Det}\left(\Sigma^{\uparrow}\right) \mathrm{Det}\left(\Sigma^{\downarrow}\right)$$

- $U(R)$ is a (two-body + three-body + . . .) correlation factor ("pseudopotential")
- $\Sigma^{\uparrow}$ is a Slater determinant of single electron orbitals $\theta_k(\vec{x}_i, \sigma_i|S)$.
- The nodes are determined by the form of the orbitals only. They are the most important part of the trial function since the nodes are not optimized by projection.
  Dense hydrogen
  - metallic state: plane waves in terms of bare or dressed coordinates (backflow)
  - molecular state: molecular orbitals (LCAO or any other reasonable form)
  - transition region: band structure or LDA self-consistent orbitals.

Trial wave functions: $|\Psi_T>$

- Slater-Jastrow form

$$\Psi_T(R|S) = \exp\left[-U(R|S)\right] \mathrm{Det}\left(\Sigma^{\uparrow}\right) \mathrm{Det}\left(\Sigma^{\downarrow}\right)$$

- $U(R)$ is a (two-body + three-body + . . .) correlation factor ("pseudopotential")
- $\Sigma^{\uparrow}$ is a Slater determinant of single electron orbitals $\theta_k(\vec{x}_i, \sigma_i|S)$.
- The nodes are determined by the form of the orbitals only. They are the most important part of the trial function since the nodes are not optimized by projection.
  Dense hydrogen
  - metallic state: plane waves in terms of bare or dressed coordinates (backflow)
  - molecular state: molecular orbitals (LCAO or any other reasonable form)
  - transition region: band structure or LDA self-consistent orbitals.
- It is possible, in principle, to systematically improve any trial function within the Feynman-Kac formalism [Holzmann et al. PRE 68, 046707 (2003)].

Backflow-3body trial functions

$$\Psi_T(\vec{R}|S) = det(e^{i\vec{k}_i\cdot\vec{x}_j})exp\left(-\sum_{i=1}^{N_e}\left[\frac{1}{2}\sum_{j\neq i}^{N_e}\tilde{u}_{ee}(r_{ij}) - \sum_{j=1}^{N_p}\tilde{u}_{ep}(r_{ij}) - \frac{1}{2}\vec{G}(i)\cdot\vec{G}(i)\right]\right)$$

backflow:

$$\vec{x}_i = \vec{r}_i + \sum_{j\neq i}^{N_e}\eta_{ee}(r_{ij})(\vec{r}_i - \vec{r}_j) + \sum_{j=1}^{N_p}\eta_{ep}(r_{ij})(\vec{r}_i - \vec{r}_j)$$

$$\eta_\alpha(r) = \lambda_b^\alpha exp[-(r/w_b^\alpha)^2]$$

3body:

$$\mathbf{G}(i) = \sum_{j\neq i}^{N_e}\xi_{ee}(r_{ij})(\vec{r}_l - \vec{r}_j) + \sum_{j=1}^{N_p}\xi_{ep}(r_{ij})(\vec{r}_i - \vec{r}_j)$$

$$\tilde{u}_{ee}(r) = u_{ee}(r) - \xi_{ee}^2(r)r^2$$

$$\tilde{u}_{ep}(r) = u_{ep}(r) - \xi_{ep}^2(r)r^2$$

$$\xi(r) = \lambda_T^\alpha exp[-(r/w_T^\alpha)^2]$$

Trial wave functions: $|\Psi_T>$

Dependence of energy on wavefunction

3d Electron fluid at a density $r_s=10$

Kwon, Ceperley, Martin, Phys. Rev. ***B58****,6800, 1998*

- Wavefunctions
  - Slater-Jastrow (SJ)?
  - three-body (3)
  - backflow (BF)
  - fixed-node (FN)
- Energy $<\phi\ |H|\ \phi>$ converges to ground state
- Variance $<\phi\ [H-E]^2\ \phi>$ to zero.
- Using 3B-BF gains a factor of 4.
- Using DMC gains a factor of 4.

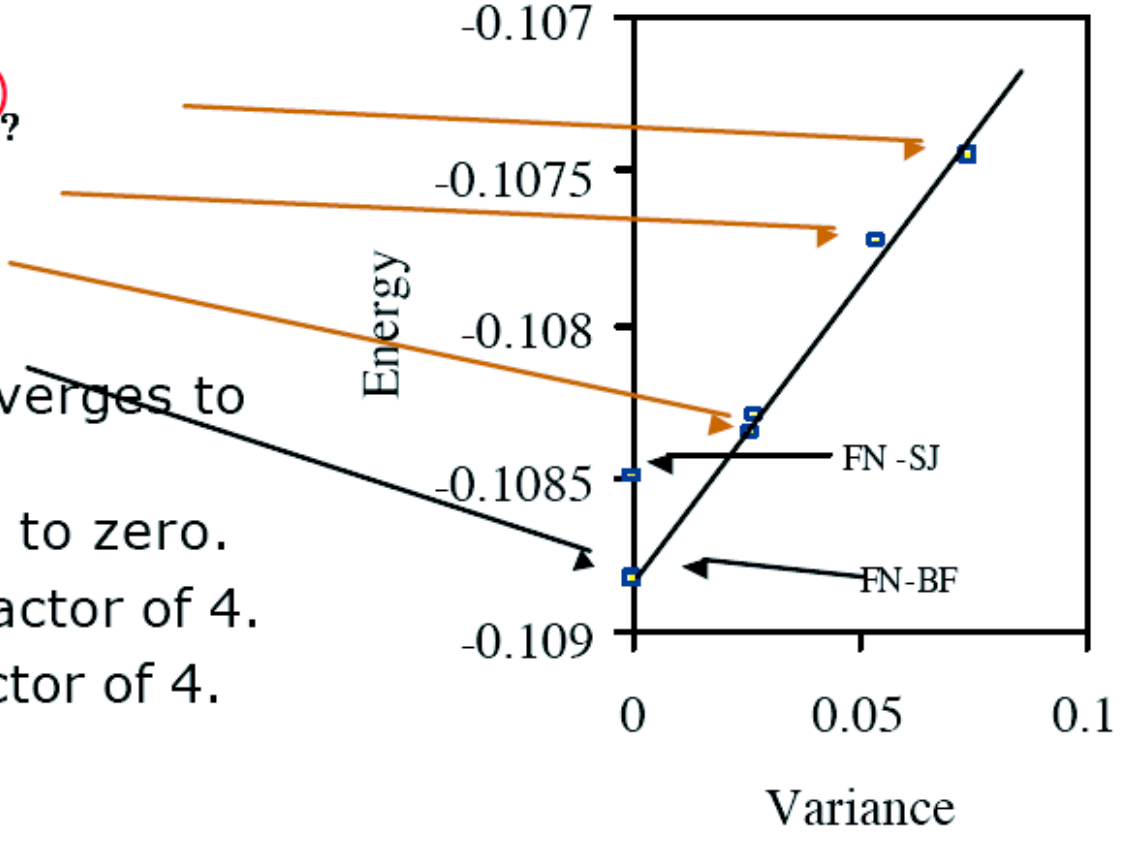

Optimization

- The optimization step in VMC can be tedious and difficult if one needs to use complex wave functions (multideterminantal, with many adjustable parameters).
- It is a non-linear optimization process: it is possible to get stuck in local minima.
- Correlated sampling improves the efficiency with respect to independent runs:
  - Set the initial condition for the parameters: $\vec{\alpha} = \vec{\alpha}_0$. Generate and store N_c statistically uncorrelated configurations (several thousands) distributed according to $|\Psi_T(R|\vec{\alpha}_0)|^2 / \int |\Psi_T(R|\vec{\alpha}_0)|^2$
  - Use your favorite minimizer for energy or the variance (or better a linear combination of them). Use reweighting to estimate the new averages

$$E_T(\vec{\alpha}) = \sum_{i=1}^{N_c} \left[\frac{\hat{H}\Psi(R_i|\vec{\alpha})}{\Psi(R_i|\vec{\alpha})} \right] w_i(\vec{\alpha}, \vec{\alpha}_0)$$

$$w_i(\vec{\alpha}, \vec{\alpha}_0) = \left| \frac{\Psi_T(R_i|\vec{\alpha})}{\Psi_T(R_i|\vec{\alpha}_0)} \right|^2 \Big/ \sum_{j=1}^{N_c} \left| \frac{\Psi_T(R_j|\vec{\alpha})}{\Psi_T(R_j|\vec{\alpha}_0)} \right|^2$$

  - Check the number of effective configurations $N_{eff} = \left(\sum_j w_j\right)^2 / \sum_j w_j^2$ remains large. Otherwise stop and regenerate the configurations with the last value of $\vec{\alpha}$.

Metallic hydrogen trial function

Metallic hydrogen: We derived analytic expressions for the backflow and 3body functions which provides as good as the trial wf with LDA orbitals but are much faster to use (Holzmann et al. PRE 68, 046707 (2003)).

No variational parameters to adjust!!

at least 5 times faster than with band orbitals

extremely useful in CEIMC

N_p		E_{VMC}(h/at)	σ^2	E_{DMC}
16	LDA	-0.4870(10)		-0.4890(5)
	BF3-O ep	-0.4857(1)	0.0317 (5)	-0.4900 (1)
	BF-A	-0.4850(1)	0.0232(1)	-0.4905(1)
54	LDA	-0.5365(5)		-0.5390(5)
	BF3-O ep	-0.5331 (6)	0.033 (1)	-0.5381 (1)
	BF-A	-0.5323(1)	0.0222(2)	-0.5382(1)
128	LDA	-0.4962(2)		-0.4978(2)
	BF3-O ep	-0.4934 (2)	0.035 (2)	-0.4958 (3)
	BF-A	-0.4928(2)	0.030(1)	-0.4978(4)

r_s=1.31, T=0K, BCC proton crystal, zero phase. (LDA=Natoli et al PRL 1993)

Two level sampling

Since the electronic part is much more expensive than computing any classical effective potential, in CEIMC we can use two level Metropolis sampling to improve the efficiency. Suppose $V_{cl}(S)$ is a reasonable proton-proton potential. The equilibrium distribution can be written as:

$$P(S) \propto e^{-\beta[E_{BO}(S)-V_{cl}(S)]}e^{-\beta V_{cl}(S)} = P_2(S)P_1(S)$$

A trial move is proposed and accepted or rejected based on a classical potential

$$A_1 = \min\left[1, \frac{T(S \to S')}{T(S' \to S)} \exp(-\beta[V_{cl}(S') - V_{cl}(S)])\right]$$

Two level sampling

Since the electronic part is much more expensive than computing any classical effective potential, in CEIMC we can use two level Metropolis sampling to improve the efficiency. Suppose $V_{cl}(S)$ is a reasonable proton-proton potential. The equilibrium distribution can be written as:

$$P(S) \propto e^{-\beta[E_{BO}(S)-V_{cl}(S)]}e^{-\beta V_{cl}(S)} = P_2(S)P_1(S)$$

A trial move is proposed and accepted or rejected based on a classical potential

$$A_1 = \min\left[1, \frac{T(S \to S')}{T(S' \to S)} \exp(-\beta[V_{cl}(S') - V_{cl}(S)])\right]$$

If we accept at the first level, the QMC energy difference is computed and the move accepted with probability

$$A_2 = \min\left[1, \exp(-\beta\Delta E_{BO} - u_B) \exp(\beta[V_{cl}(S') - V_{cl}(S)]\right]$$

where u_B is the noise penalty.

Quantum protons

- By increasing pressure or decreasing temperature, ionic quantum effects start to become relevant. Those effects are important for hydrogen at high pressure.

Quantum protons

- By increasing pressure or decreasing temperature, ionic quantum effects start to become relevant. Those effects are important for hydrogen at high pressure.
- Static properties of quantum systems at finite temperature can be obtained with Path Integral Monte Carlo method (PIMC).
  We need to consider the thermal density matrix rather than the classical Boltzmann distribution:

$$\rho_P(S, S'|\beta) = < S|e^{-\beta(K_p + E_{BO})}|S' >$$

  The same formalism as in RQMC applies. However
  1 - β is the physical inverse temperature now.
  2 - to compute averages of diagonal operators we map quantum protons over ring polymers
  3 - we limit to distinguishable particle ($T > T_d$).

Quantum protons

- By increasing pressure or decreasing temperature, ionic quantum effects start to become relevant. Those effects are important for hydrogen at high pressure.
- Static properties of quantum systems at finite temperature can be obtained with Path Integral Monte Carlo method (PIMC).
  We need to consider the thermal density matrix rather than the classical Boltzmann distribution:

$$\rho_P(S, S'|\beta) =< S|e^{-\beta(K_p+E_{BO})}|S' >$$

  The same formalism as in RQMC applies. However
  1 - β is the physical inverse temperature now.
  2 - to compute averages of diagonal operators we map quantum protons over ring polymers
  3 - we limit to distinguishable particle ($T > T_d$).
- Factorization $\beta = P\tau_p$ and Trotter break-up
  For efficiency introduce an effective proton-proton potential $\hat{H}_{eff} = \hat{K}_P + \hat{V}_{eff}$

$$\hat{\rho}_P(\tau_p) = e^{-\tau_p[\hat{H}_{eff}+(\hat{E}_{BO}-\hat{V}_{eff})]} \approx e^{-\tau_p\hat{H}_{eff}}e^{-\tau_p[\hat{E}_{BO}-\hat{V}_{eff}]}$$

Quantum protons - 2

- We compute numerically the matrix elements of the effective pair density matrix $\hat{\rho}^{(2)}_{eff}(\tau_p)$ (see lecture notes). The effective N-body density matrix is approximated by

$$< S|\hat{\rho}^{(N)}_{eff}(\tau_p)|S' > \approx \prod_{ij} < s_i, s_j|\hat{\rho}^{(2)}_{eff}(\tau_p)|s_i, s_j > + O(n^3)$$

Quantum protons - 2

- We compute numerically the matrix elements of the effective pair density matrix $\hat{\rho}^{(2)}_{eff}(\tau_p)$ (see lecture notes). The effective N-body density matrix is approximated by

$$< S|\hat{\rho}^{(N)}_{eff}(\tau_p)|S' > \approx \prod_{ij} < s_i, s_j|\hat{\rho}^{(2)}_{eff}(\tau_p)|s_i, s_j > +O(n^3)$$

- We add the remaining term of the original Hamiltonian $(E_{BO} - V_{eff})$ at the level of the primitive approximation.

Quantum protons - 2

- We compute numerically the matrix elements of the effective pair density matrix $\hat{\rho}^{(2)}_{eff}(\tau_p)$ (see lecture notes). The effective N-body density matrix is approximated by

$$< S|\hat{\rho}^{(N)}_{eff}(\tau_p)|S' > \approx \prod_{ij} < s_i, s_j|\hat{\rho}^{(2)}_{eff}(\tau_p)|s_i, s_j > +O(n^3)$$

- We add the remaining term of the original Hamiltonian $(E_{BO} - V_{eff})$ at the level of the primitive approximation.
- With this Trotter break-up we found convergence to the continuum limit ($\tau_p \longrightarrow 0$) for $1/\tau_p \geqslant 3000K$ which allows to simulate systems at room temperature with only $M \approx 10$ proton slices (for metallic hydrogen at $r_s = 1$).

Quantum protons - 3

In CEIMC quantum protons are almost for free !

- Suppose we run classical ions with a given level of noise $(\beta\sigma_{cl})^2$. Consider now representing the ions by P time slices. To have a comparable extra-rejection due to the noise we need a noise level per slice given by: $(\tau_p\sigma_k)^2 \approx (\beta\sigma_{cl})^2/P$ which provides $\sigma_k^2 \approx P\sigma_{cl}^2$. We can allow a noise per time slice P times larger which means considering P times less independent estimates of the energy difference per slice. However we need to run P different calculations, one for each different time slice, so that the amount of computing for a fixed global noise level is the same as for classical ions.

Quantum protons - 3

In CEIMC quantum protons are almost for free !

- Suppose we run classical ions with a given level of noise $(\beta\sigma_{cl})^2$. Consider now representing the ions by P time slices. To have a comparable extra-rejection due to the noise we need a noise level per slice given by: $(\tau_p\sigma_k)^2 \approx (\beta\sigma_{cl})^2/P$ which provides $\sigma_k^2 \approx P\sigma_{cl}^2$. We can allow a noise per time slice P times larger which means considering P times less independent estimates of the energy difference per slice. However we need to run P different calculations, one for each different time slice, so that the amount of computing for a fixed global noise level is the same as for classical ions.
- When using TABC, for any proton time slice we should in principle perform a separate evaluation of the BO energy difference averaging over all phases. We have checked that, at each proton step, we can randomly assign a subset of phases at each time slice and get the same results.

Quantum protons - 3

In CEIMC quantum protons are almost for free !

- Suppose we run classical ions with a given level of noise $(\beta\sigma_{cl})^2$. Consider now representing the ions by P time slices. To have a comparable extra-rejection due to the noise we need a noise level per slice given by: $(\tau_p\sigma_k)^2 \approx (\beta\sigma_{cl})^2/P$ which provides $\sigma_k^2 \approx P\sigma_{cl}^2$. We can allow a noise per time slice P times larger which means considering P times less independent estimates of the energy difference per slice. However we need to run P different calculations, one for each different time slice, so that the amount of computing for a fixed global noise level is the same as for classical ions.
- When using TABC, for any proton time slice we should in principle perform a separate evaluation of the BO energy difference averaging over all phases. We have checked that, at each proton step, we can randomly assign a subset of phases at each time slice and get the same results.
- We need to move all slices of all protons together. This limits the length of proton paths, therefore the temperature we can achieve. It is essential to use the best possible Trotter factorization!!

Summary of CEIMC

- Given an initial configuration of the electronic path Q and the protonic path P, propose a trial protonic move P' with a suitable transition probability (depending on the particular system).

Summary of CEIMC

- Given an initial configuration of the electronic path Q and the protonic path P, propose a trial protonic move P' with a suitable transition probability (depending on the particular system).
- Assign at random an equal number of twist phases to any proton slice and run many independent electronic calculations for each twist phase: ideal for parallel computers !

Summary of CEIMC

- Given an initial configuration of the electronic path Q and the protonic path P, propose a trial protonic move P' with a suitable transition probability (depending on the particular system).
- Assign at random an equal number of twist phases to any proton slice and run many independent electronic calculations for each twist phase: ideal for parallel computers !
- Sample the electronic configuration space with the importance sampling distribution depending on both P and P'.

Summary of CEIMC

- Given an initial configuration of the electronic path Q and the protonic path P, propose a trial protonic move P' with a suitable transition probability (depending on the particular system).
- Assign at random an equal number of twist phases to any proton slice and run many independent electronic calculations for each twist phase: ideal for parallel computers !
- Sample the electronic configuration space with the importance sampling distribution depending on both P and P'.
- Use reweighting to compute energy difference Δ and variance σ^2 by averaging results over all twist phases and proton slices

Summary of CEIMC

- Given an initial configuration of the electronic path Q and the protonic path P, propose a trial protonic move P' with a suitable transition probability (depending on the particular system).
- Assign at random an equal number of twist phases to any proton slice and run many independent electronic calculations for each twist phase: ideal for parallel computers !
- Sample the electronic configuration space with the importance sampling distribution depending on both P and P'.
- Use reweighting to compute energy difference Δ and variance σ^2 by averaging results over all twist phases and proton slices
- Performe the Metropolis test with the penalty method

Summary of CEIMC

- Given an initial configuration of the electronic path Q and the protonic path P, propose a trial protonic move P' with a suitable transition probability (depending on the particular system).
- Assign at random an equal number of twist phases to any proton slice and run many independent electronic calculations for each twist phase: ideal for parallel computers !
- Sample the electronic configuration space with the importance sampling distribution depending on both P and P'.
- Use reweighting to compute energy difference Δ and variance σ^2 by averaging results over all twist phases and proton slices
- Performe the Metropolis test with the penalty method
- Compute average quantities for the old protonic configuration P using reweighting.

High pressure hydrogen

- Analytical backflow-3body trial wavefunctions
- Systems of up to 54 quantum protons and 54 unpolarized electrons
- VCM vs RQMC
- CEIMC vs Restricted PIMC
- CEIMC vs LDA-CPMD (Kohanoff 1995).
- Proton quantum effects
- Data for the Equation of State and for correlation functions.
- Melting of the proton crystal with temperature by the dynamical transition and Lindemann criterium.
- Molecular phase: CEIMC vs experimental data
- Molecular dissociation in liquid state: preliminary results

VMC vs RQMC

r_s=1.31, N_p=N_e=16, θ=2π(0.4,0.5,0.6)

fixed pair of protonic configurations, 1000 blocks of 40000 esteps

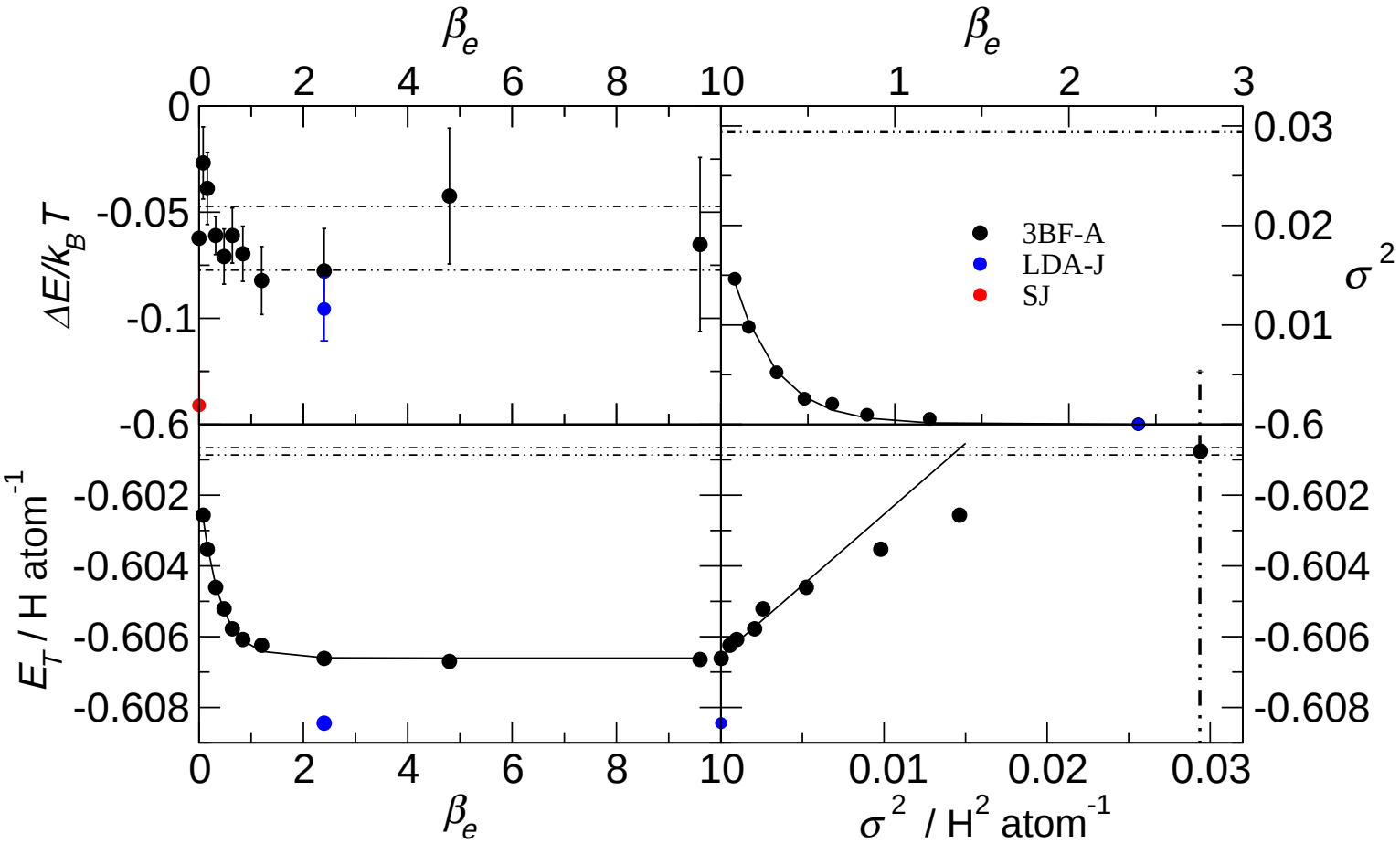

$$E_{RQMC} - E_{VMC} = 5.7mH/at = 1810K/at$$

Metallic Hydrogen: VMC vs RQMC

r_s=1.2, T=5000K, N_p=54, zero phase.

- RQMC gives total energy lower by 7.6(2)mH/at=2400(60)K/at
- RQMC pressure is 0.03Mbars lower than VMC (0.5%)

τ_e	E_{tot}(h/at)	σ^2	E_{kin}	E_{pot}	P (Mbars)
vmc	-0.4694(2)	0.0472(4)	0.8812(4)	-1.3508(4)	5.55(1)
0.01	-0.4768(4)	—	0.8850(6)	-1.3618(6)	5.50(1)
0.00	-0.47696	—	0.89112	-1.36808	5.581

- CPU time for RQMC $\simeq$ 10 $\times$(CPU time for VMC)

Metallic Hydrogen: VMC vs RQMC

r_s=1.2, T=5000K, N_p=54, zero phase

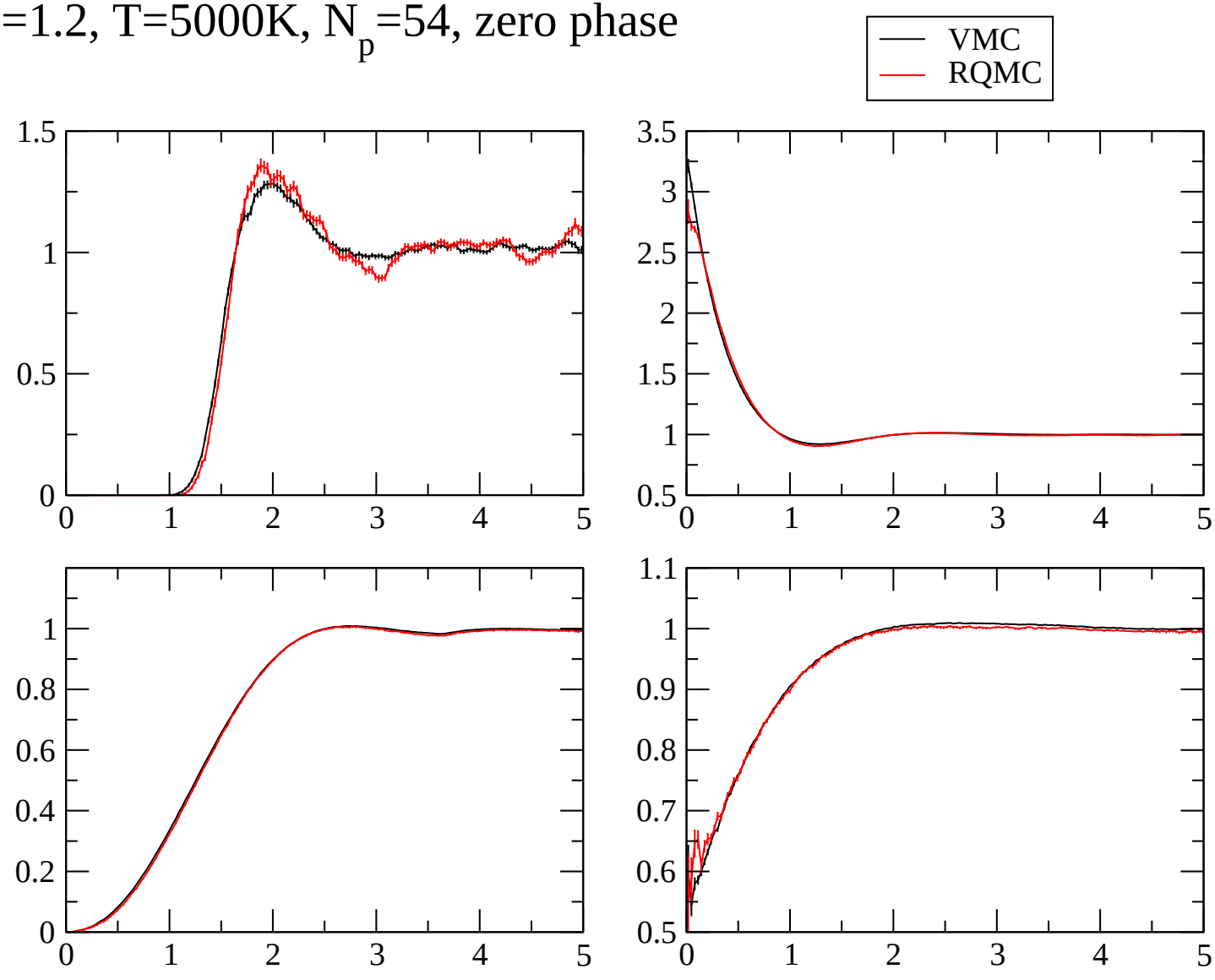

Metallic Hydrogen: VMC vs RQMC

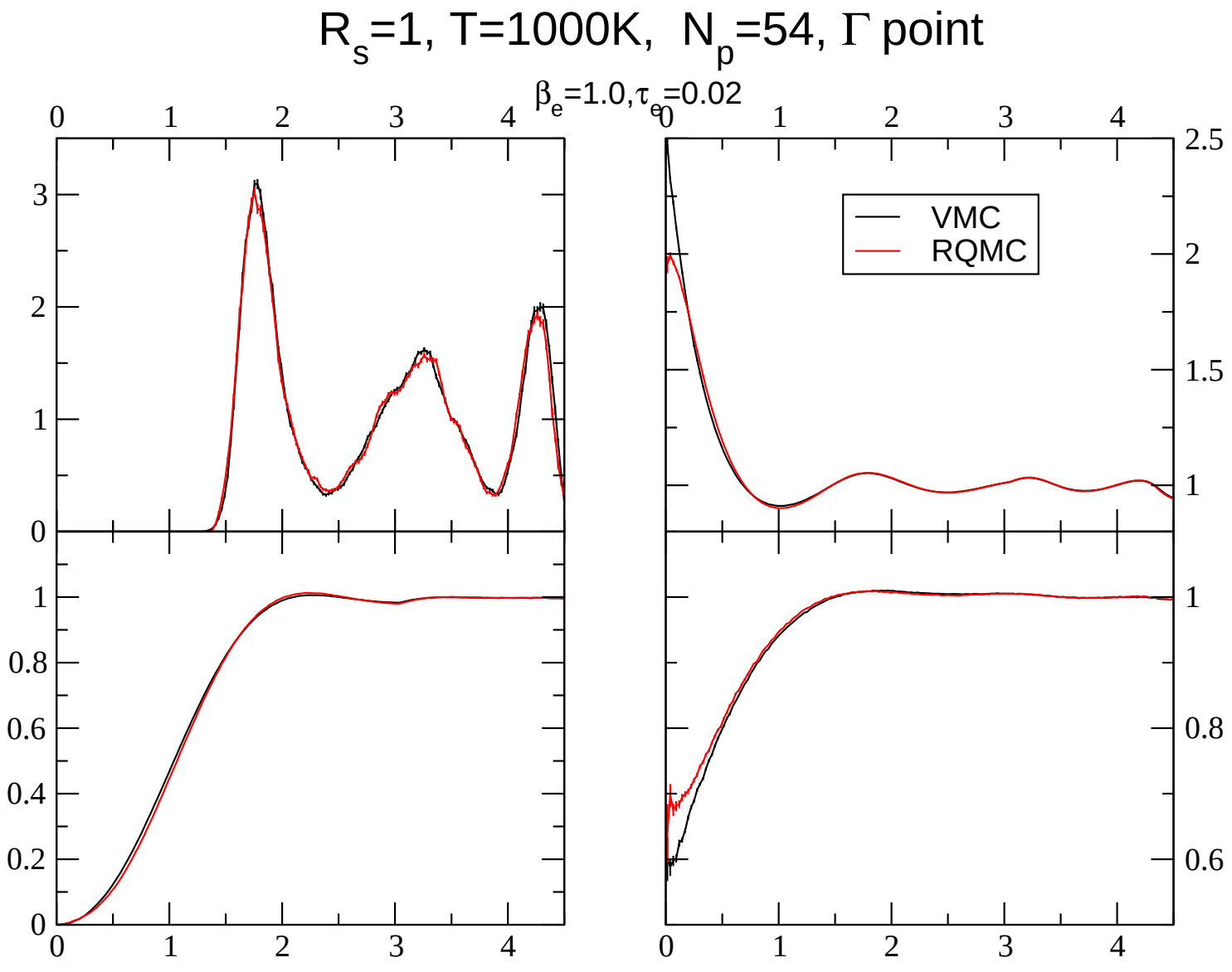

CEIMC vs Restricted PIMC

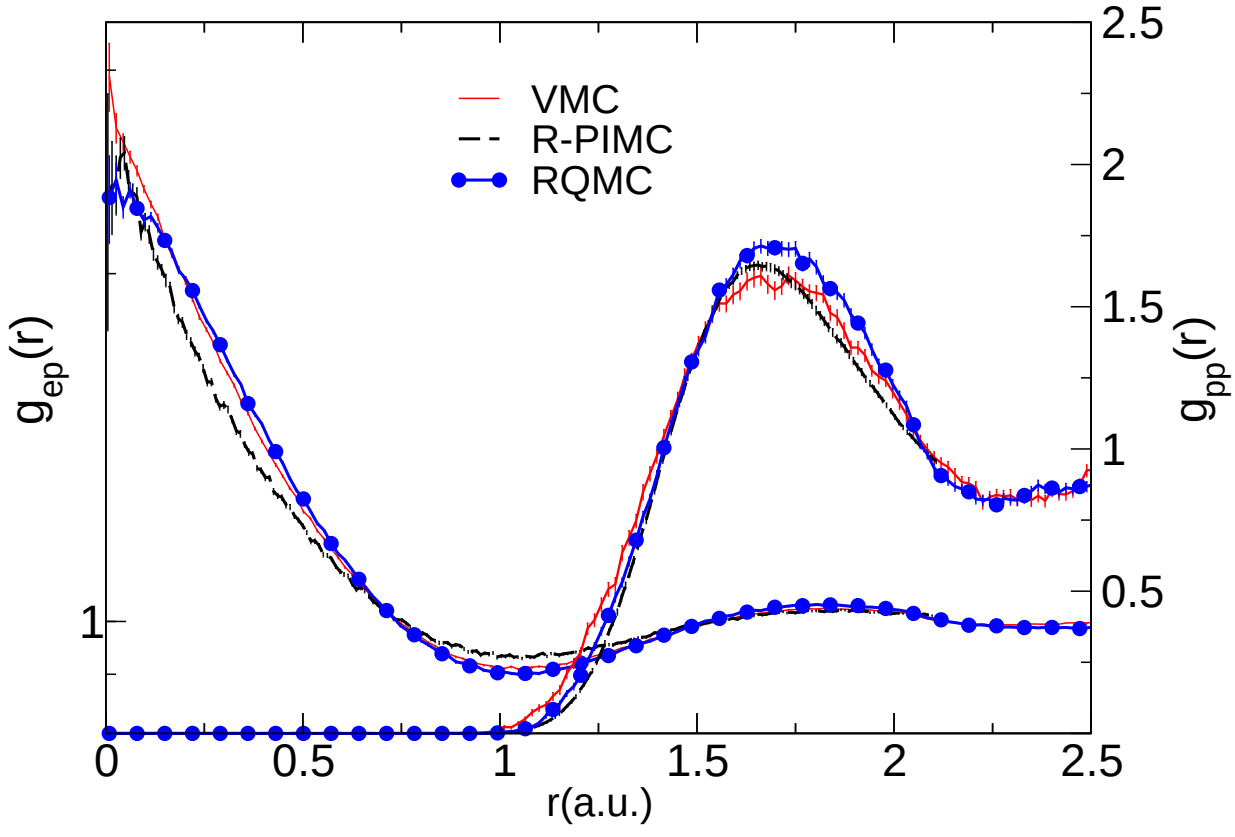

CEIMC vs RPIMC for electron-proton and proton-proton correlation function at $r_s = 1, T = 5000K, N_p = N_e = 16$, Γ point. RPIMC has ground state free particle nodes.

CEIMC vs LDA-CPMD

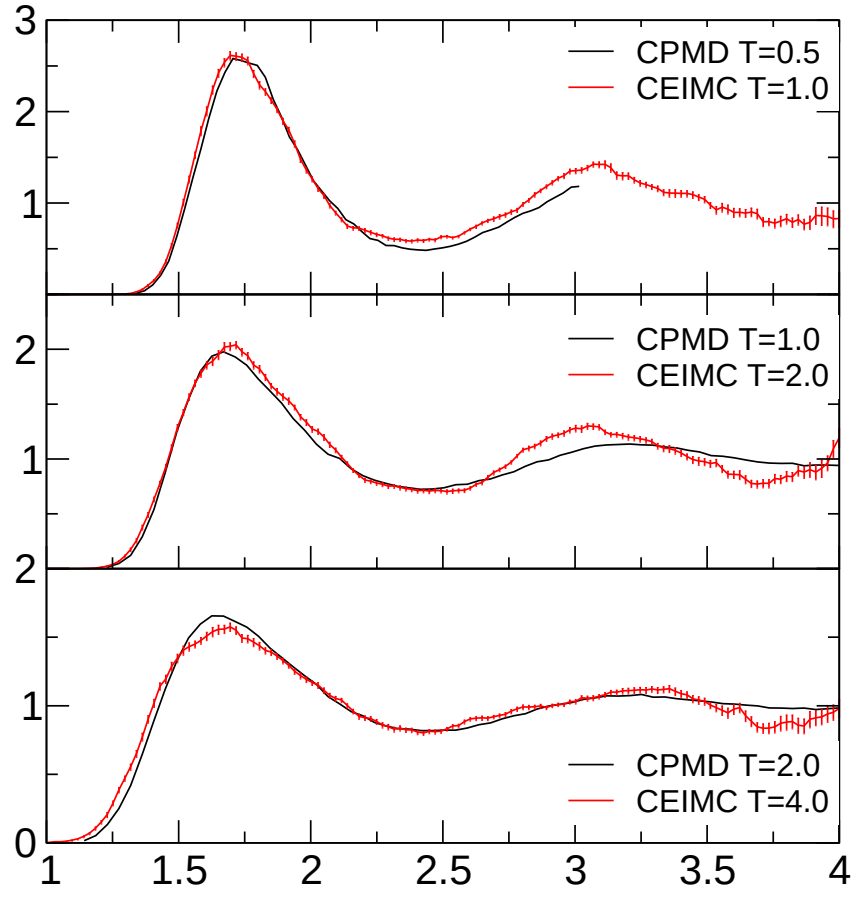

- LDA predicts less structure than observed in CEIMC.
- Proton melting:
  - $T_m(LDA) \simeq 350K$ (Lindemann ratio) (Kohanoff 1995)
  - $1000K \leq T_m(CEIMC) < 1500K$ (dynamical criterium)

QMC vs LDA

TABLE I. The static and dynamic LDA, VMC, and DMC energies, for the d
zero point energy, virial pressure, and Lindemann's ratio.

	E_{LDA} (Ry)	E_{VMC} (Ry)	E_{DMC} (Ry)
			Static
bcc	−1.01392	−1.0062(3)	−1.0101(3)
Simple cubic	−1.01898	−1.0144(4)	−1.0185(3)
Simple hexagonal	−1.02406	−1.0275(4)	−1.032(1)
Diamond	−1.02413	−1.0204(4)	−1.0235(2)
β-Sn	−1.02711	−1.022(1)	−1.0256(7)
			Dynamic
bcc		−0.9716(1)	−0.9810(7)
Simple cubic		−0.9747(1)	−0.9873(3)
Simple hexagonal		−0.9828(2)	−0.988(1)
Diamond		−0.9821(2)	−0.993(1)
β-Sn		−0.981(1)	−0.992(2)

Ground state energies for several crystal structures of atomic hydrogen. Comaprison between QMC and LDA. From Natoli, Martin and Ceperley, PRL **70**, 1952 (1993).

- QMC energy differences are about twice the corresponding LDA ones.

QMC vs LDA

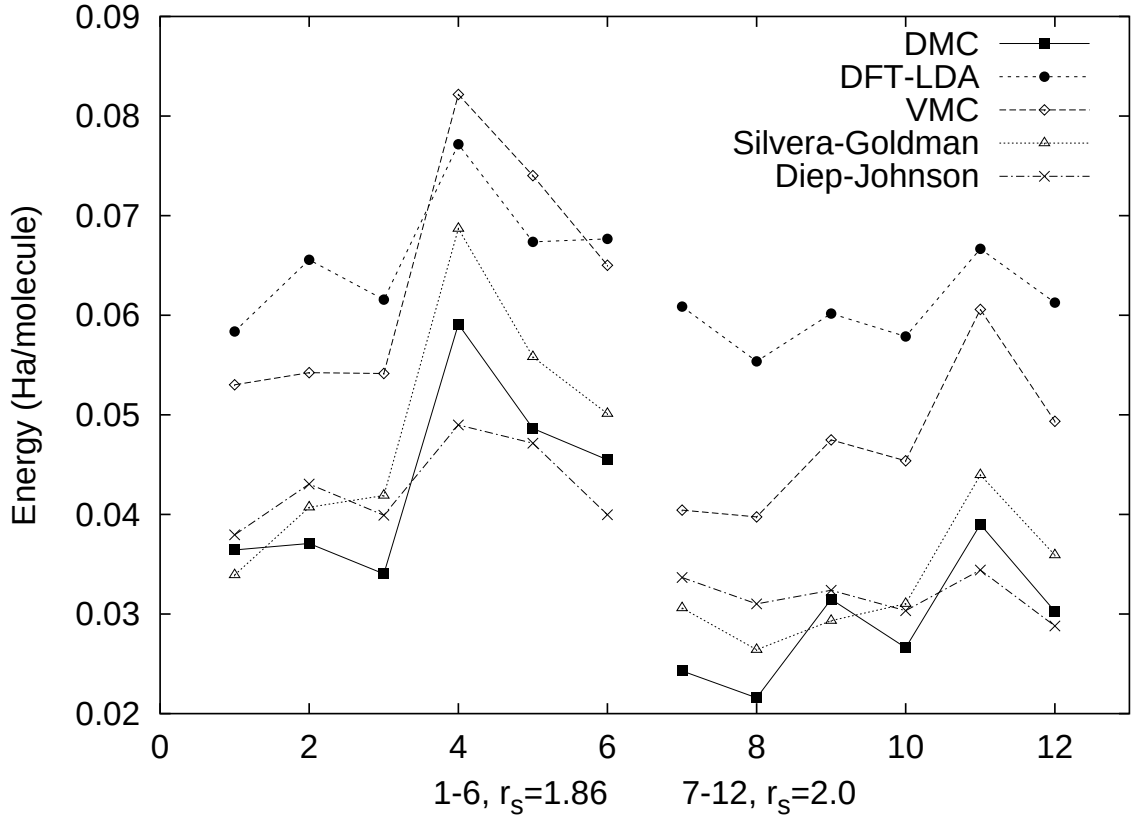

Electronic energy for several configurations computed by various methods. The energy is relative to an isolated H_2 molecule (from Mark Dewing).

- QMC energy differences are about 1.5 times larger than LDA ones.

Atomic Metallic Hydrogen: EOS

- r_s=1.2: $5.90 \leq P \leq 7.69$ Mbars
- r_s=1.0: $20.68 \leq P \leq 23.53$ Mbars
- r_s=0.8: $81.95 \leq P \leq 86.66$ Mbars

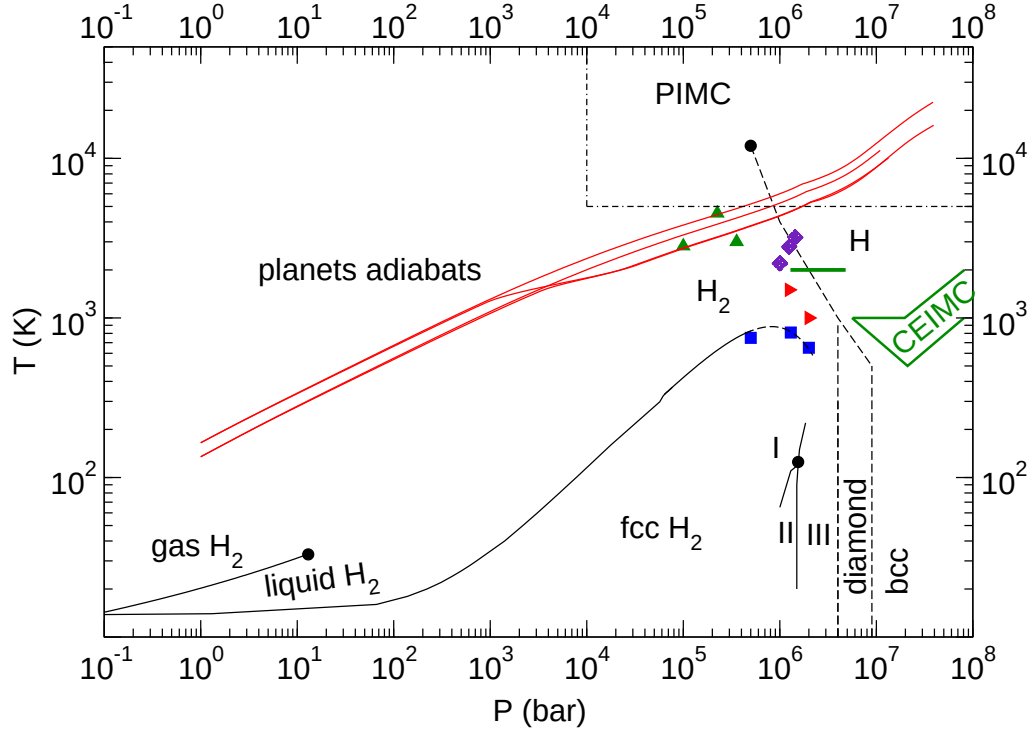

- Effects of ZPM on the melting line are small.

Proton quantum effects

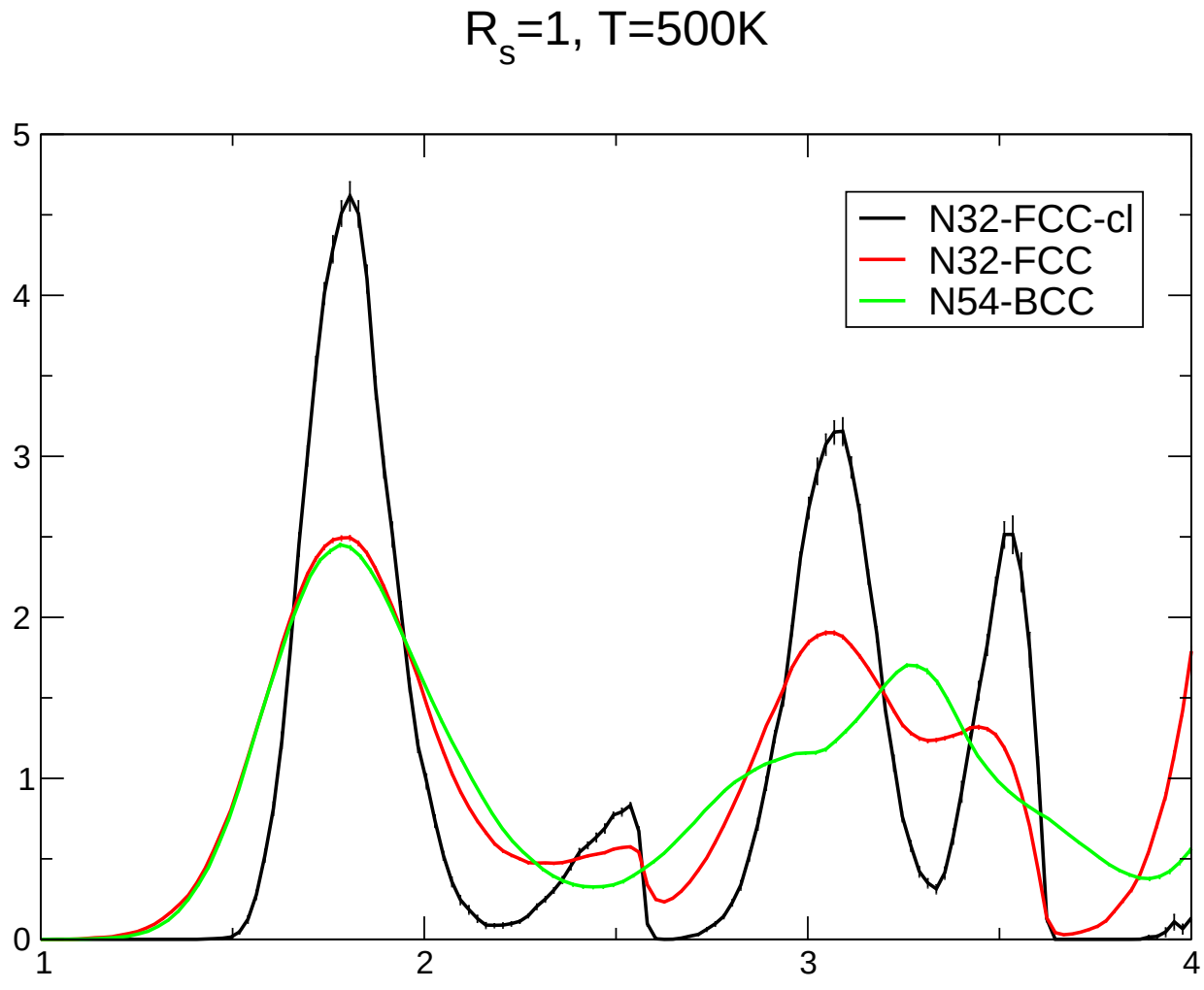

Proton quantum effects

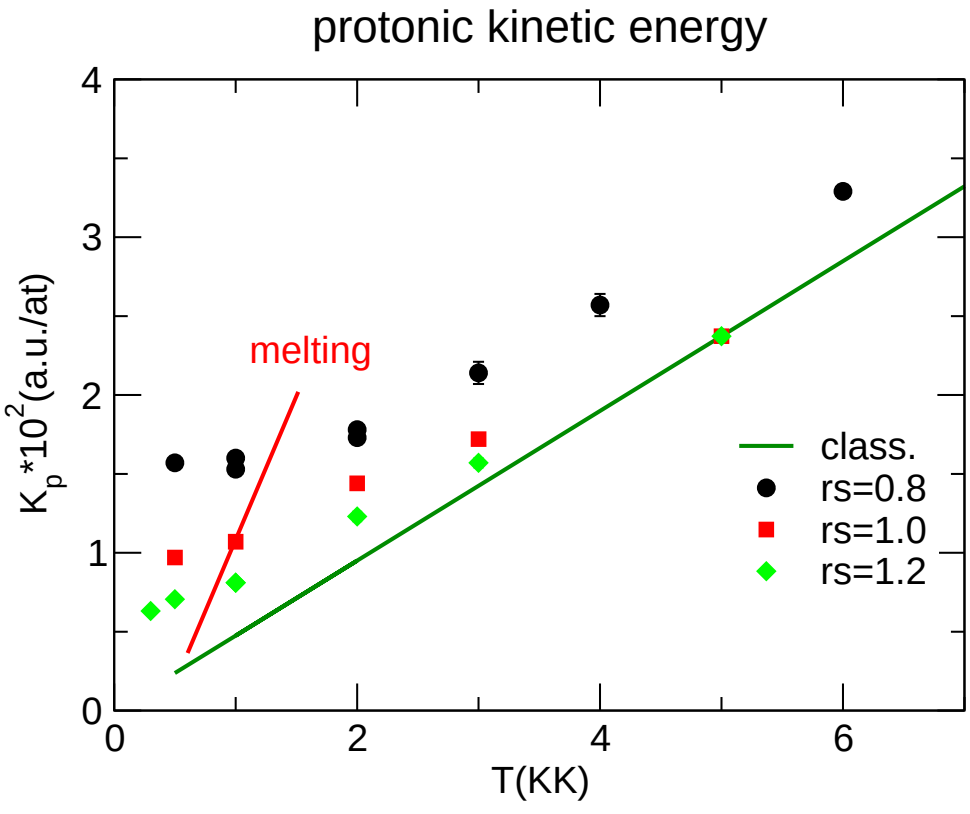

$N_e = N_p = 54$ spin unpolarized. Proton kinetic energy per particle at various densities versus temperature. The red line is the estimated melting line for the bcc crystal from the Lindemann ratios.

Proton quantum effects

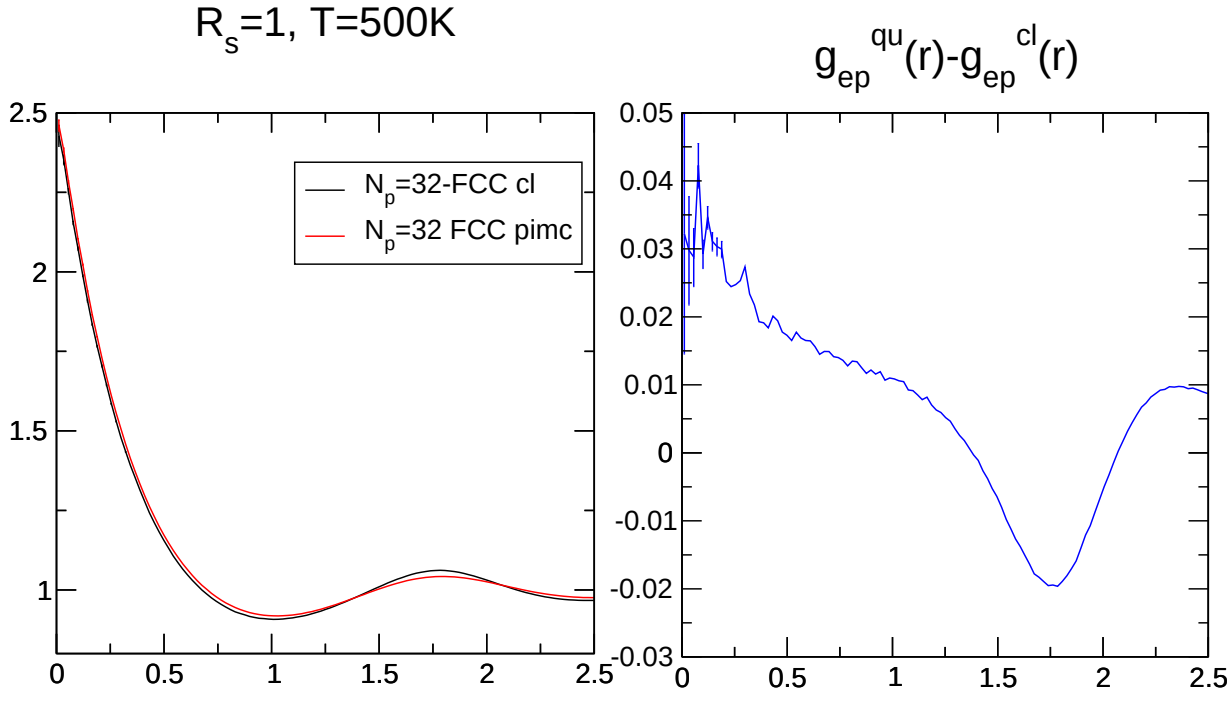

- Quantum protons change electronic properties:

$$E_{tot}(qu) - E_{tot}(cl) = 14.9(2) mH/at = 4670(60) K/at$$

$$K_p(qu) - K_p(cl) = 2020(30) K/at$$

$$\Delta E_{tot} - \Delta K_p = \begin{cases} 450(10) K/at & : \quad configurational\ (Coulomb) \\ 2200(20) K/at & : \quad electronic\ kinetic\ energy \end{cases}$$

Main conclusions

- we have developed an efficient method for treating electron-nuclei systems with QMC accuracy within the Born-Oppenheimer approximation
- LDA seems to fail not only in predicting gaps (metalization) but even in predicting the correct liquid state and the melting line at least in the metallic phase (known problems also in other systems).

- # Main conclusions
  - we have developed an efficient method for treating electron-nuclei systems with QMC accuracy within the Born-Oppenheimer approximation
  - LDA seems to fail not only in predicting gaps (metalization) but even in predicting the correct liquid state and the melting line at least in the metallic phase (known problems also in other systems).
- # In progress
  - insulating molecular hydrogen: comparison with experiments and prediction of the EOS, including the melting line.
  - molecular-atomic transition in liquid phase (LLPT)

Insulating Molecular Hydrogen

r_s=2.1, T=4.53KK, N_p=54

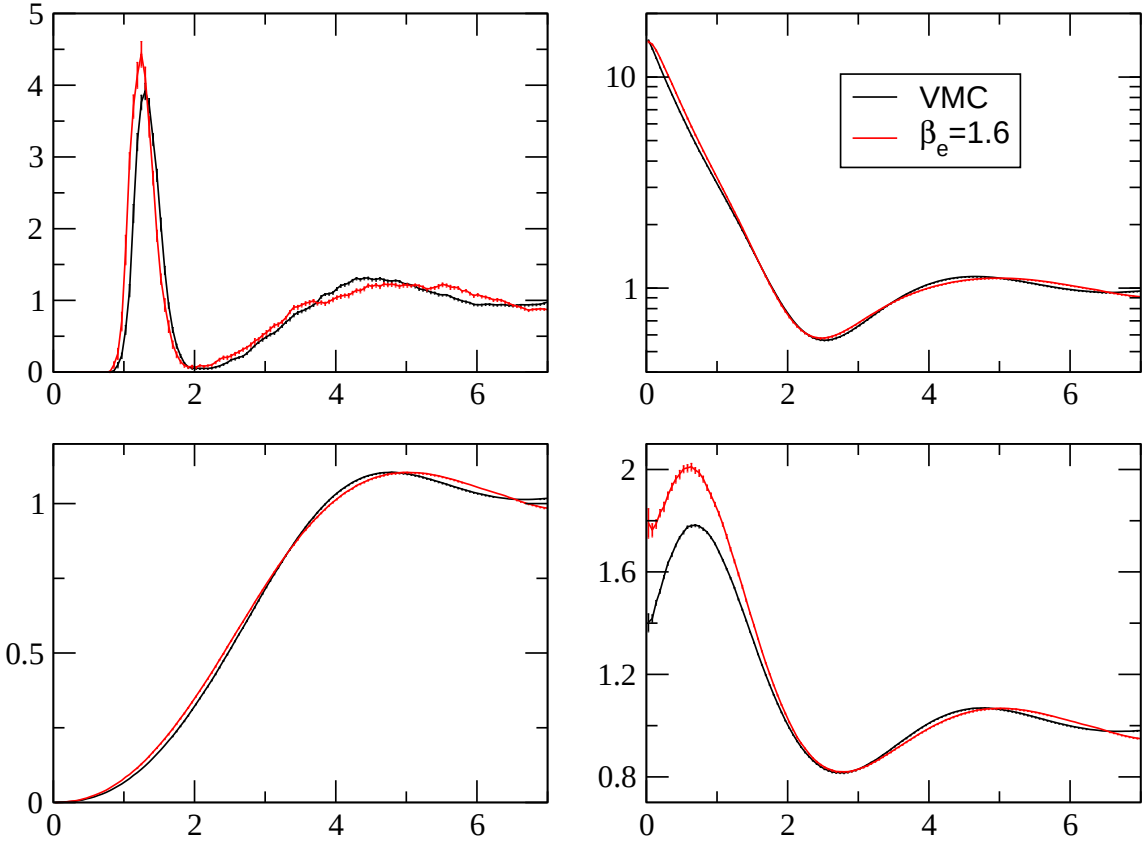

LCAO: one guassian center on each proton of the molecule. A single variational parameter

P_{VMC}=0.149(2)Mbars, P_{RQMC}=0.224(5)Mbars, $P_{gas-gun}$=0.234Mbars

We still don't have quantum protons here ! sorry

Molecular Hydrogen: Liquid-Liquid PT

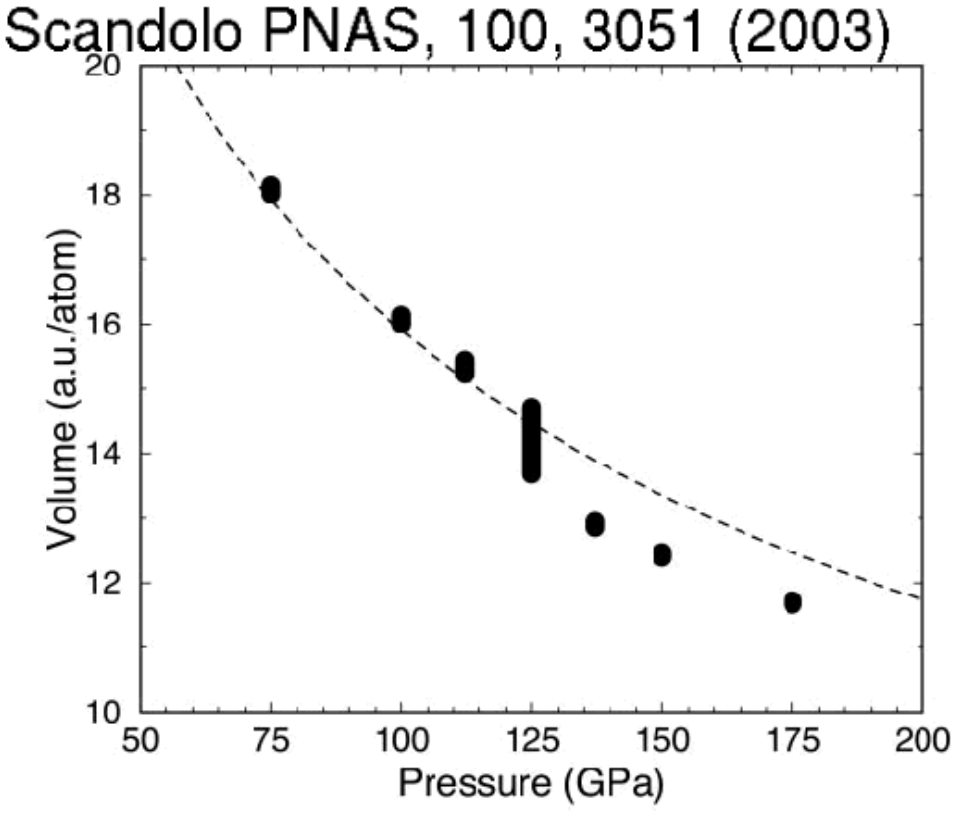

Fig. 1. Calculated volumes for liquid hydrogen at 1,500 K (bars; their size gives the error). The anomalous error bar at 125 GPa is discussed in the text. The dashed line indicates the experimental volume at 300 K (23).

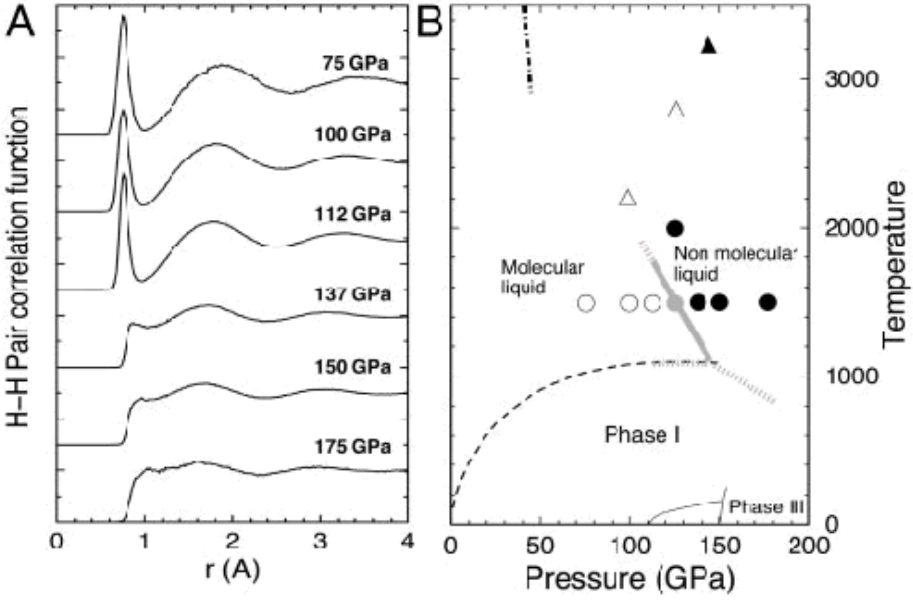

Fig. 2. (*A*) Pair correlation functions of hydrogen at 1,500 K and the pressures indicated. (*B*) Sketch of the hydrogen phase diagram. Circles indicate points where simulations were performed; ○ correspond to points where the system was found to be molecular (nonmolecular points are indicated by ●). Triangles indicate shock-wave points from ref. 2. A continuous transition from insulating (△) to metal (▲) behavior was observed. The dashed line is an extrapolation of the melting line (7). The dash-dotted line is an extrapolation of the first-order transition line predicted by quantum Monte Carlo simulations with free-particle nodes for the electronic wave function (24). Gray lines indicate suggested phase boundaries.

Liquid-Liquid PT: CEIMC

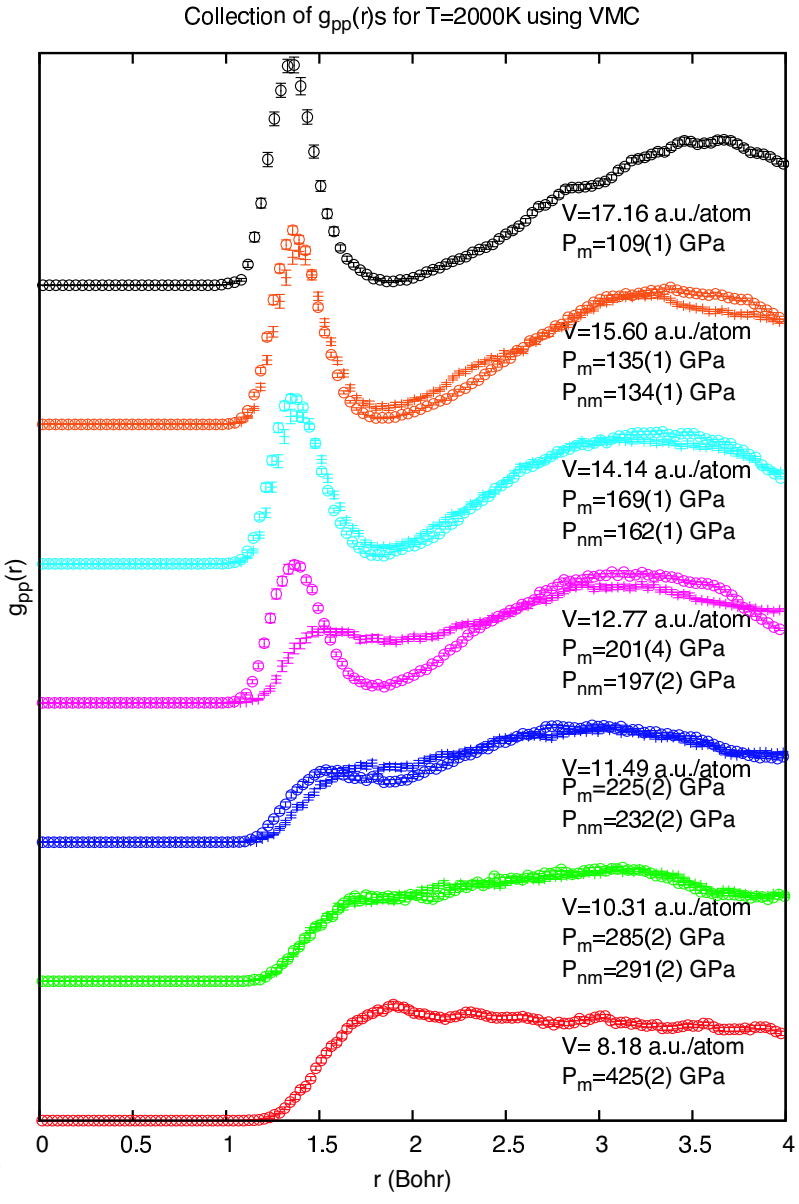

Molecular dissociation in the warm liquid

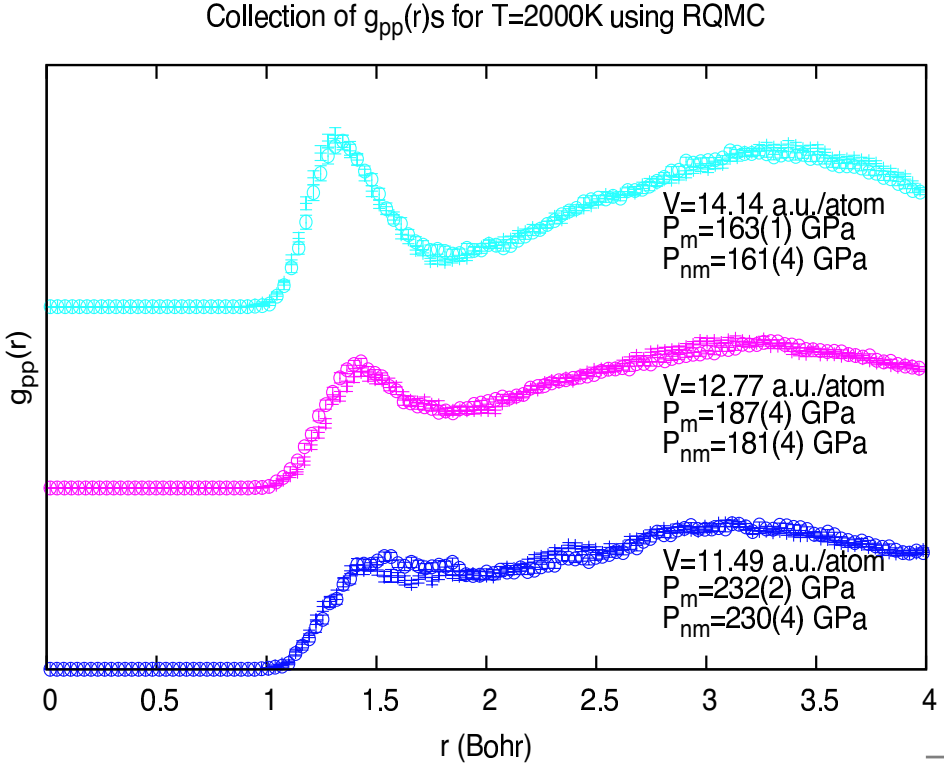

Future developments

- Constant-pressure algorithm to directly investigate structural phase transitions (level crossing problem).
- Study the melting of the molecular solid in the insulating phase (recent experiments and theoretical prediction of a maximum in T vs P transition line, Bonev, Nature 2004).
- Investigate the possibility of a high pressure-low temperature liquid phase before the appearance of the atomic crystal
- Introduce the use of pseudopotentials to extend the method to heavier elements.

Related publications

1. D.M. Ceperley, M. Dewing and **C. Pierleoni** “The coupled Electronic-Ionic Monte Carlo simulation method”, Lecture Notes in Physics, vol 605, pp 473-499, Springer Verlag (2002), physics/0207006.
2. M. Holzmann., D.M.Ceperley, **C. Pierleoni** and K. Esler “Backflow correlation in the electron gas and metallic hydrogen” *Phys. Rev. E* **68**, 046707 (2003, USA).
3. **C. Pierleoni**, D.M. Ceperley and M. Holzmann “Coupled Electron-Ion Monte Carlo Calculations of Dense Metallic Hydrogen”, *Phys. Rev. Lett.* **93**, 146402 (2004), physics/0405056.
4. M. Holzmann, **C. Pierleoni** and D.M. Ceperley, “Zero-point energy of atomic hydrogen by Coupled Electron-Ion Monte Carlo Method”, *Computer Physics Communications* **169**, 421 (2005).
5. **C. Pierleoni** and D.M. Ceperley: “Computational Methods in Coupled Electron-Ion Monte Carlo”, *CHEMPHYSCHEM* **6**, 1872-1878 (2005).
6. **C. Pierleoni** and D.M. Ceperley: “The coupled Electron-Ion Monte Carlo method”, to appear in *Lecture Notes in Physics* (2006).